To the Graduate Council:

I am submitting herewith a dissertation written by Mary Anne Kozilsky Moore entitled "The Nonlinear Optical Response of Sodium Vapor when Pumped to a Two-Photon Resonance." I have examined the final copy of this dissertation for form and content and recommend that it be accepted in partial fulfillment of the requirements for the degree of Doctor of Philosophy, with a major in Physics.

John O. Thomson, Major Professor

We have read this dissertation
and recommend its acceptance:

Accepted for the Council:

Vice Provost
and Dean of the Graduate School

THE NONLINEAR OPTICAL RESPONSE OF SODIUM VAPOR WHEN PUMPED TO A TWO-PHOTON RESONANCE

A Dissertation

Presented for the

Doctor of Philosophy

Degree

The University of Tennessee, Knoxville

Mary Anne Kozilsky Moore

August 1988

ACKNOWLEDGEMENTS

Few scientific endeavors have ever been the product of a sole investigator, and this has certainly not been one of them. Without the help of several individuals this study would never have been completed. Special thanks must go to Ray Garrett and Marvin Payne whose patience and guidance have been invaluable. The technical assistance of both Steve Allman and Ron Phillips has kept the experiments running despite many potential long-term technical delays. Each member of the Photophysics Group at ORNL has helped at one time or another and to all these people I offer my sincere thanks.

ABSTRACT

Although the nonlinear response of sodium vapor to intense laser stimulation has been an active topic over the last three decades, many of the phenomena associated with the two-photon excitation of resonance states have not been fully understood. This study examines primarily three aspects of the nonlinear process associated with the two-photon excitation of either the sodium 3d or 4d states. The first is the suppression of forward hyper-Raman emission due to interference with four-wave mixing emission, and is an extension of previous theoretical and experimental work done in inert gases by the Chemical Physics Section of Oak Ridge National Laboratory.

The second topic is the suppression of backward stimulated hyper-Raman emission due to the a.c. Stark effect. The medium itself generates a near resonance emission that, in turn, generates an electric field of sufficient intensity to cause a shifting of the resonance outside the bandwidth of the incident laser. This has the effect of decreasing the gain for the hyper-Raman process.

The last major section of this study involves the discovery of a new type of process, axially phase-matched four-wave mixing. Normal four-wave mixing emission propagates only in the direction of the laser beam. To phase match in a pure vapor it must propagate conically rather than down the axis of the incident laser beam. This study has shown that four-wave mixing may take advantage of the

dispersive properties of the sodium vapor near resonances to index match and propagate coherently down the axis of the laser beam rather than adjusting its cone angle to phase match. Although observations of some of the phenomena reported in this study have been reported in the literature, this is the first time that many of them have been explained satisfactorily in terms of the nonlinear response of sodium atoms.

TABLE OF CONTENTS

LIST OF FIGURES

FIGURE PAGE

FIGURE PAGE

LIST OF ACRONYMS, ABBREVIATIONS, AND CONVERSION FACTORS

$\mathring{A}$	Angstrom
ASE	Amplified stimulated emission
FWM	Four-wave mixing
IR	Infrared
PFWM	Parametric four-wave mixing
SHR	Stimulated hyper-Raman
SRE	Stimulated Raman emission
UV	Ultraviolet
δ	Detuning from resonance
Δ_s	a.c. Stark shift

$1\ \mathring{A} = 10^{-8}$ cm

$1\text{W} = 10^{7}$ erg/sec

$1\ \text{cm}^{-1} \equiv 1.986 \times 10^{-16}$ ergs $= 1.986 \times 10^{-23}$ J

$$\frac{1}{\lambda}\,[\text{cm}^{-1}] = \frac{E}{hc}\,\frac{[\text{ergs}]}{[\text{erg-sec}][\frac{\text{cm}}{\text{sec}}]}$$

CHAPTER I

INTRODUCTION

The field of nonlinear optics has been an active area of research since the early 1960s when the advent of lasers introduced light sources with high enough power density to produce measurable nonlinear effects. The motivation to study resonantly enhanced nonlinear optical processes has had many sources. Most of the early studies were done in solids where the crystal structure provided an asymmetry that allowed for the production of lowest order nonlinear processes such as second harmonic generation. Since lower order processes are generally stronger than higher order ones, these effects were easier to produce.

Nonlinear processes in crystals and gaseous media allow the production of light at frequencies not available from a conventional laser source. The production of this light was one of the earliest practical results derived from nonlinear optical studies. This avenue of research has led to an extensive increase in the spectral range of coherent frequency sources. An interest in nonlinear effects in metallic vapors and gases was motivated by the desire to learn more about atomic and molecular systems, and to make use of sharp resonances to greatly enhance processes of low probability. It is with this application that the following studies deal.

In the usual treatment of nonlinear optics, as typified by Bloembergen's classic text Nonlinear Optics (1965), processes are described through the higher order susceptibility terms in the expansion of the polarization of a medium in a power series in the applied electric field, $\vec{E}$.

$$\vec{P} = \chi^{(1)} \cdot \vec{E} + \chi^{(2)} : \vec{E}\,\vec{E} + \chi^{(3)} \vdots \vec{E}\,\vec{E}\,\vec{E} + \ldots \qquad (1.1)$$

where $\vec{P}$ is the polarization or electric dipole moment per unit volume of the medium, and $\chi^{(n)}$ is the nth order electric susceptibility tensor. $\chi^{(n)}$ is a dimensionless constant. Higher order susceptibility terms have very complex forms that have been worked out very carefully by theorists in the field such as Shen et al. (1984).

In the traditional susceptibility treatment of nonlinear optical phenomena the higher order electric susceptibility terms are evaluated for each nonlinear process. In even powered higher order susceptibility expressions, all terms cancel completely if spherical symmetry exists in the nonlinear media. Specifically, $\chi^{(2)}$, the lowest order nonlinear term in the expansion of the polarization in Eq. (1.1), is nonzero only in a medium where no inversion symmetry exists (Shen et al., 1984). This limited early nonlinear studies to solids because laser energies available at that time were insufficient to produce measurable nonlinear effects involving higher orders than $\chi^{(2)}$.

In a gas or vapor spherical symmetry exists so that the lowest order nonzero nonlinear term in the expansion of Eq. (1.1) is $\chi^{(3)}$.

Many researchers in the field (for example: Agarwal, 1984; Payne and Garrett, 1980 and 1986; and Hanna, 1979) have found that the susceptibility treatment is not practical when applied to resonantly enhanced nonlinear processes in gases or vapors. This is because the expansion in Eq. (1.1) is only justified if there is negligible population transfer between states in the medium (Hanna, 1979). Instead these investigators use the polarization at other frequencies as source terms in Maxwell's equations and then apply time-dependent perturbation theory. The sources for these other frequencies become evident if one defines the time dependence of the electric field vector in Eq. (1.1), $\vec{E}$, in terms of exponentials such as $\vec{E} = \vec{E}_0(e^{+i\omega t} + e^{-i\omega t})$. For example, consider the second term in Eq. (1.1) with two electric fields at frequencies ω_1 and ω_2. The second order term in the polarization expansion then has terms from the product of the exponential terms

$$(e^{+i\omega_1 t} + e^{-i\omega_2 t}) \text{ and } (e^{+i\omega_2 t} + e^{-i\omega_2 t}) .$$

The frequencies produced are $\pm(\omega_1 + \omega_2)$ and $\pm(\omega_1 - \omega_2)$. For each resulting sum or difference frequency, there are three frequencies in the medium, ω_1, ω_2, and the generated frequency. This type of process is often referred to as three-wave mixing. If $\omega_1 = \omega_2$, the sum frequency is just twice the initial frequency; this is called second harmonic generation.

This analogy will be carried on to the third order term, since many of the effects studied in later chapters are directly related to

this term in the expansion. To more carefully align this discussion to the experiments that follow, the most general case (three fields at three different frequencies) will not be used. Instead, it is assumed that two of the fields are degenerate in frequency (this corresponds to the two-photon resonance referred to in the title of this dissertation). A second frequency, ω_2, is introduced either externally or produced by some process in the medium itself. The exponential terms involved in this case are:

$$(e^{+i\omega_1 t} + e^{-i\omega_1 t})^2 (e^{+i\omega_2 t} + e^{-i\omega_2 t}) .$$

The resulting frequencies include $2\omega_1 \pm \omega_2$. These are referred to as sum or difference frequencies depending on the sign. Four fields are involved in the process, two at ω_1, one at ω_2, and the sum or difference frequency, $2\omega_1 \pm \omega_2$. Therefore, this is called a four-wave mixing process. The process of interest in this study is four-wave difference mixing, and it will be explained in more detail later.

The specific studies described in these experiments were motivated by earlier work done by the Chemical Physics Section at Oak Ridge National Laboratory with the nonlinear response of xenon. Their success in theoretically modeling the effects of pulsed laser stimulation on the production of third harmonic light and the suppression of resonantly enhanced ionization due to four-wave mixing, lead to a desire to explain some of the nonlinear wave mixing behavior seen in alkali metals, sodium in particular. Describing nonlinear behavior in sodium proved to be a much more complex problem

than in xenon because the one-photon resonant enhancement possible in the alkali metals does not exist in the noble gases. However, progress has been made. The rest of this chapter deals with the common elements of the experiments described in the following chapters. These include a brief sketch of the nonlinear optics, a description of the energy levels of the sodium atom, the laser system, the heat pipe used to contain the sodium vapor, and a brief description of the types of emission expected.

A. A Brief Sketch of Nonlinear Optics

The response of an atomic system (in this particular case, the sodium atom) to an external electromagnetic field can be described to a very good approximation through the electric dipole interaction. The Hamiltonian of the system is then written as

$$H = H_0 - \hat{D} \cdot \vec{E} \tag{1.2}$$

where H_0 represents the unperturbed atomic system, $\vec{E}$, the electric field vector of the external electromagnetic field, and $\hat{D}$ is the dipole operator, $-e\vec{r}$, where e is the charge on an electron. The Hamiltonian is written without spin because the spin of the outer electron of the alkali atom does not play a direct role in this process in the electric dipole approximation. The macroscopic polarization can be written as $\vec{P} = N < \psi_r(t)|\hat{D}|\psi_r(t) >$ where $\psi_r(t)$ is the wave function for the atomic system and N is the number density

of atoms in the nonlinear medium. As already shown, the nonlinear polarization has terms at different frequencies. The polarization at a given frequency may then be used as a source term in the wave equation for that frequency (Shen et al., 1984). For a neutral vapor (so that $\vec{\nabla} \cdot \vec{E} = 0$):

$$\nabla^2 \vec{E}(\omega) - \frac{1}{v^2} \frac{\partial^2 \vec{E}(\omega)}{\partial t} = \frac{4\pi}{c^2} \frac{\partial^2 \vec{P}^{NL}(\omega)}{t^2} \qquad (1.3)$$

where $\vec{E}(\omega)$ is the electric field vector generated at the new frequency, ω, v is the phase velocity of the generated wave, c is the speed of light in a vacuum, and $\vec{P}^{NL}(\omega)$ is the nonlinear polarization at ω. The present study experimentally examines the generation of these nonlinear polarizations and the electromagnetic waves that result from them. In addition, it examines the factors which influence these processes when two or more occur simultaneously.

B. The Sodium Atom

The experiments described in the following chapters were conducted in sodium vapor and were directed toward understanding the total atomic response in an optically dense medium when an intense laser beam is tuned through a two-photon allowed transition. A medium is optically dense when some absorption of the incident laser beam occurs when the frequency of the laser is at some allowed resonance frequency. The response studied is not specific to sodium vapor, but may apply to many vapors and gases. Sodium was chosen because the energy levels of the sodium atom may be resonantly

excited by frequencies that are readily produced in the laser systems available. In addition, the frequencies produced by nonlinear processes in sodium are in a wavelength region that is easily monitored by available detectors.

In the present case, nonlinear processes associated with near-resonant transitions to either the 3d or 4d states are investigated (see Figure 1.1). Because of parity and angular momentum considerations not all states are coupled by one-photon transitions. If both states have either odd or even parity they may only be connected (in the dipole approximation) by even numbers of photons. Odd number photon transitions are allowed only between states of opposite parity. All the experiments that follow explore the atomic response of a collection of sodium atoms pumped by a pulsed laser beam tuned to frequencies corresponding to near or exact two-photon resonances from the 3s ground state to either the 3d or 4d states. The d states are separated by a small fine structure splitting into a $d_{5/2}$ and $d_{3/2}$ doublet. However, in these studies it is not possible to resolve $3d_{5/2,3/2}$ or $4d_{5/2,3/2}$ splittings due to the finite size of the bandwidth of the available lasers. The widths of the fine structure splittings of the 3d and 4d states are 0.04 cm^{-1} and 0.035 cm^{-1}, respectively (Moore, 1971). The 0.04 cm^{-1} bandwidth of the dye laser is insufficient to resolve these fine structure levels. Consequently, unless selection rules mandate otherwise, these doublets are treated as a single level. The fine structure splitting in the p states involved in these experiments (either $3p_{3/2,1/2}$ or

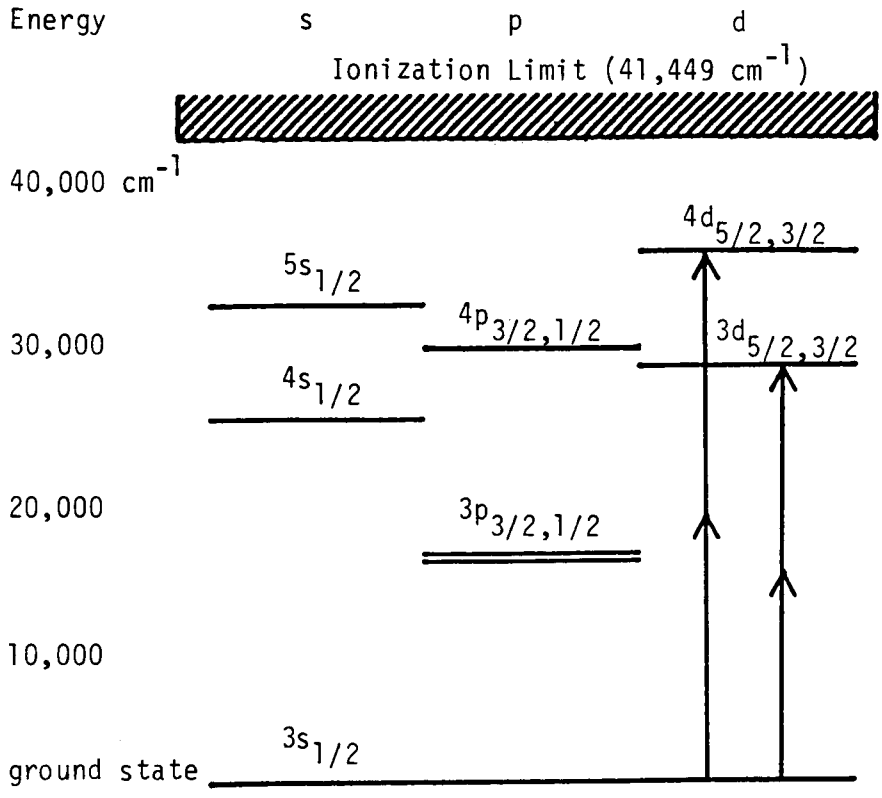

Figure 1.1. Available energy levels for the sodium atom up to the 4d states (Weise et al., 1969). Processes that result from two-photon pumping of the 3d or 4d states are studied.

$4p_{3/2,1/2}$) are sufficiently wide to resolve them as separate states [13.2 cm^{-1} and 5.6 cm^{-1}, respectively (Moore, 1971)]. Since s and d states both have even parity the laser frequency is adjusted so that the energy of two laser photons $2\hbar\omega_L$ = E(3s-4d) or E(3s-3d). The strength of the transition between various states can be gauged by the oscillator strength (F_{ij}) between those states. The oscillator strengths for a large number of atomic sodium transitions have been compiled by the National Bureau of Standards, and the ones of interest are listed in Table 1.1 (Weise et al., 1969).

One of the properties of an atomic vapor which is determined by the oscillator strengths of relevant transitions is the dispersion of the vapor in given frequency regions (Born and Wolf, 1975). This property becomes important in Chapter IV when examining phase matching between imposed and generated electromagnetic waves for certain processes, and will be discussed in more detail there.

C. The Heat Pipe and Laser System

Two pieces of equipment are common to the present experiments: a heat pipe to contain the sodium vapor, and a tunable pulsed laser to excite the sodium atoms.

How does one contain a metallic vapor in a particular volume of space in a way that will still allow a laser beam or beams at other frequencies produced by the nonlinear medium to pass through it? One answer is to use a heat pipe (see Figure 1.2). Sodium metal is heated in a region in the middle of the heat pipe where it is

Table 1.1. Sodium Transition and Associated Oscillator Strengths Connected to the Two-Photon Excitation of the Sodium 4d and 3d Levels (Weise et al., 1969, Except where Noted)

Transition (l - u)	(Å)	$F_{\ell,u}$
$3s_{1/2}$-$3p_{3/2}$	5889.95	0.640 ± 3%[a]
$3s_{1/2}$-$3p_{1/2}$	5895.92	0.3178 ±.17%[b]
$3p_{3/2}$-$4d_{5/2}$	5788.21	0.095 ± 18%
$3p_{3/2}$-$4d_{3/2}$	5688.19	0.0106 ± 18%
$3p_{1/2}$-$4d_{3/2}$	5682.63	0.106 ± 18%
$3s_{1/2}$-$4p_{3/2}$	3302.37	0.00878 ± 18%[a]
$3s_{1/2}$-$4p_{1/2}$	3302.98	0.00426 ± 18%[a]
$4p_{3/2}$-$4d_{5/2}$	23379.1	0.82 ± 18%
$4p_{3/2}$-$4d_{3/2}$	23379.0	0.091 ± 18%
$4p_{1/2}$-$4d_{3/2}$	23348.4	0.91 ± 18%
$4s_{1/2}$-$4p_{3/2}$	22056.4	0.9 ± 25%
$4s_{1/2}$-$4p_{1/2}$	22083.7	0.45 ± 25%
$3p_{1/2}$-$4s_{1/2}$	11381.5	0.163 ± 25%
$3p_{3/2}$-$4s_{1/2}$	11403.8	0.163 ± 25%
$3d_{5/2}$-$4p_{3/2}$	90880.0	0.117 ± 25%
$3d_{3/2}$-$4p_{1/2}$	91380.0	0.098 ± 25%
$3d_{3/2}$-$4p_{3/2}$	90880.0	0.0195 ± 25%
$3p_{3/2}$-$3d_{5/2}$	8194.82	0.75 ± 25%
$3p_{1/2}$-$3d_{3/2}$	8183.26	0.83 ± 25%
$3p_{3/2}$-$3d_{3/2}$	8194.79	0.083 ± 25%

[a]Hofsaess, 1977. [b]Gaupp, 1977.

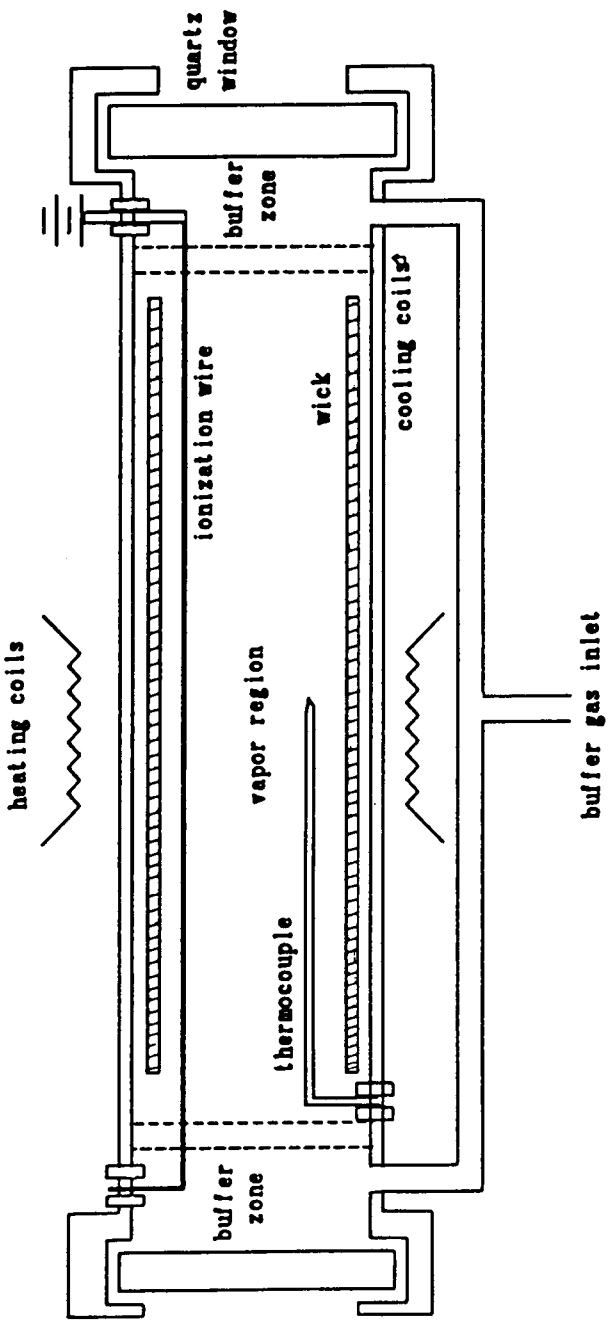

Figure 1.2. Schematic diagram of a heat pipe.

vaporized by heating coils wrapped around the body. Cooling coils at the ends of this vapor region make the sodium vapor condense out into a wire mesh "wick" where it is drawn back by capillary action to heat pipe center and revaporized. Quartz windows at the end of the heat pipe allow electromagnetic radiation to pass into and out of the vapor region. The transmission properties of quartz allow radiation from the ultraviolet region through the near infrared to pass through the heat pipe with negligible losses. The processes of interest in these studies have frequencies within this wavelength region.

To keep the windows from becoming fogged by condensed metal vapor a gas is introduced that forms a buffer region between the cooling coils and the windows. When the heat pipe is run in "heat pipe mode" the vapor pressures of the buffer gas (argon) and the sodium vapor are equal and circulating sodium vapor pushes the argon atoms to the outer regions of the heat pipe. This results in a vapor region of pure sodium vapor. The sodium vapor pressure is determined from the temperature of the vapor which is measured by a thermocouple embedded near the center of the heat pipe. The temperature is controlled by regulating the voltage applied to the heating coils. In these experiments the heat pipe was rarely, if ever, run in this mode. Instead, the argon pressure was kept above the sodium vapor pressure. This results in the vapor region having a mixture of argon and sodium atoms. At the operating temperatures used there are also small and inconsequential quantities (no more than a few percent, Gordon et al., 1971) of sodium dimers and probably mixed dimers of sodium and argon.

In some of these experiments an attempt was made to make ionization measurements of the sodium vapor. This was accomplished by having a metal charge collection wire strung along the length of the vapor region. The wire was insulated at its ends from the heat pipe and subjected to a bias voltage for collection of photoelectrons. By measuring the voltage relative to the grounded heat pipe it was hoped that one might determine the relative degree of ionization of the sodium vapor. Problems associated with space charge effects make measurements of absolute ionization yields impractical at best. In fact, it was discovered that even measurements of relative ionization efficiencies of certain processes cannot be made reliably due to space charge effects that occur even at relatively low sodium pressures and low incident laser energies. For a more detailed discussion of space charge effects, see McDaniel, 1964.

The second common piece of equipment was the laser system. When only one tunable laser beam was necessary, a Lumonics series TE-860-2 excimer-pumped dye laser was used. This excimer laser was run with a XeCl gas mixture to give a narrow band pulse of 4 to 6 ns in duration at a wavelength of 3080 Å. This light was used to pump a tunable dye laser, where the choice of dye was determined by the output frequency desired. The energy output of the pump laser depended on the dye used, but was in the range of a fraction to several millijoules per pulse. The bandwidth of this laser was 0.04 cm^{-1}. Bandwidths are given in units of inverse centimeters which are the energy units used in laser spectroscopy

(see Weise, 1965). The bandwidth given in these units remains constant over the entire frequency range of all available dyes for a particular pump laser. For each frequency produced by the dye laser, this 0.04 cm^{-1} bandwidth may be translated into a wavelength range by using the relationship:

$$0.04\ cm^{-1} = |\vec{k}_2| - |\vec{k}_1| \propto 1/\lambda_2 - 1/\lambda_1$$

where $|\vec{k}_1|$ and $|\vec{k}_2|$ represent the energy in wave numbers between the ends of the bandwidth range and λ_1 and λ_2 are the corresponding wavelengths. When the dye laser is pumping at a wavelength of 3000 Å, a bandwidth of 0.04 cm^{-1} corresponds to 0.004 Å. At a wavelength of 7000 Å, 0.04 cm^{-1} is equivalent to 0.020 Å. These wavelength spreads differ by a factor of five. This is why laser bandwidths are given in energy units that remain constant across the entire spectral range of a dye laser rather than in wavelength units that must be recalculated for each frequency. However, when discussing incident laser detunings from resonance levels in later chapters, the detuning, δ, will be given in angstroms. This is the value the experimenter reads off the scanning unit of the dye laser. The output beam had a nonuniform spatial profile that had to be taken into account in certain of the experiments.

In the experiments where two incident laser frequencies were required, a Quanta Ray Nd-Yag laser was used to pump matching dye lasers. The overall quality of these beams was far inferior to the

excimer laser. The bandwidth was $\sim$0.65 cm^{-1} and the spatial profiles of the beams were doughnut-shaped.

D. Types of Electromagnetic Emission

Certain types of electromagnetic radiation are referred to repeatedly in the experiments described in later chapters. To establish a background for later discussion, a brief description will be given of some types of emission that are possible and conditions under which they are produced.

Spontaneous emission occurs when an atom in an excited state emits a photon and drops to a lower allowed energy state. Amplified Spontaneous Emission (ASE) can only occur when there is a collection of atoms in an excited state. It is called spontaneous emission because at least one atom spontaneously emits a photon as it drops to a lower allowed energy state. However, after this atom spontaneously emits a photon, the photon can stimulate other excited atoms to also de-excite by emitting photons, and the process is said to be amplified. In this sense the process is also often called Amplified Stimulated Emission. To distinguish between spontaneous emission and absorption, and stimulated emission, see Figure 1.3. To produce ASE there must exist a system of excited atoms rather than a single isolated atom. The stimulated emission has the additional feature of being exactly in phase with the stimulating photon, and, of course, this is the basis for the lasing process. Since ASE may only occur in the spatial region containing the pump photons where

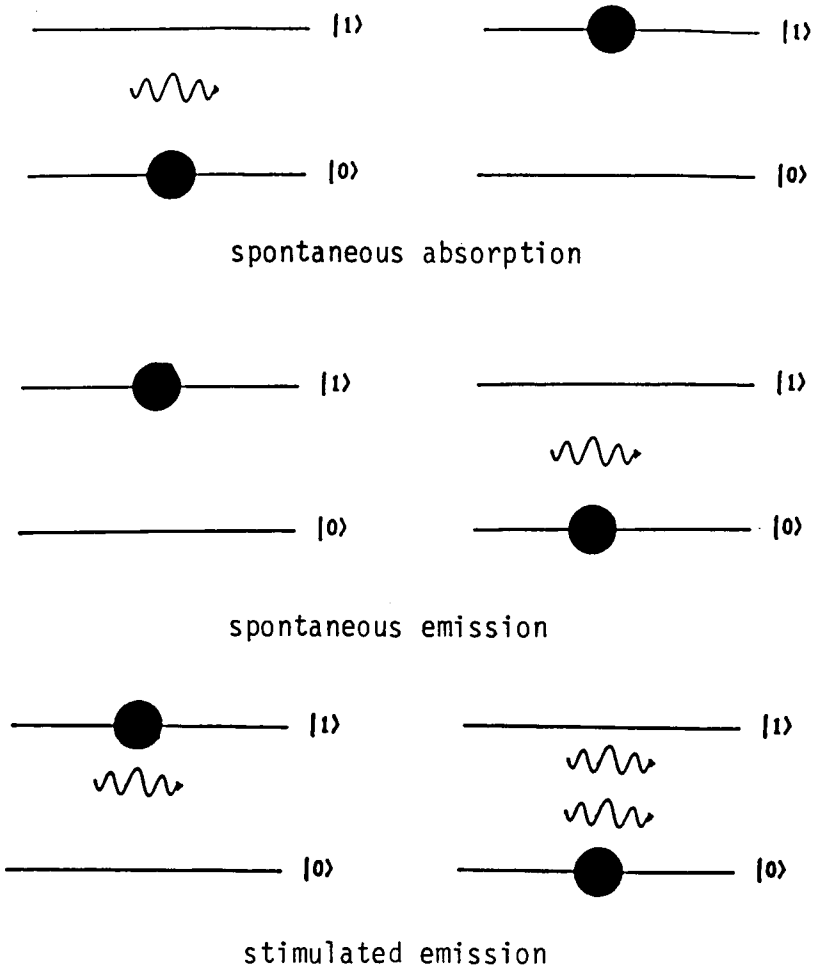

Figure 1.3. Schematic diagrams of spontaneous absorption, spontaneous emission, and stimulated emission.

excited atoms are created, one would expect ASE to occur along the incident laser beam in either the forward or backward direction. There is a definite transfer of population from a given state to the other states involved in the process. A simplified schematic of the ASE produced in the experiments through two-photon excitation can be found in Figure 1.4a. In the top schematic the laser frequency is adjusted so that the total energy of the two photons matches the energy between states $|0\rangle$ and $|2\rangle$. These states have the same parity (even in this case), and transitions between them can be induced by two photons. To simplify the example it is assumed that the bandwidth of the laser is such that it is no wider than the broadened resonance width. Electrons are transferred from the $|0\rangle$ ground state to the $|2\rangle$ state. ASE occurs when electrons in the $|2\rangle$ level de-excite by photon emission to the $|1\rangle$ level, an odd parity state.

Although Raman processes are more commonly associated with molecular transitions, they may also occur in atomic systems. Stimulated Raman Emission (SRE) is a two-photon process that involves the excitation of an atom by an externally supplied photon to a virtual state that is usually near, but not directly on, an atomic resonance, and the subsequent generation of another photon. This leads to the simultaneous excitation of an electronic transition, leaving the atom in an excited state. As with ASE, the stimulated Raman emission process may propagate in either the forward or backward direction. This is ordinary Raman scattering (or emission), a process observed in the present studies, but not one that plays a significant

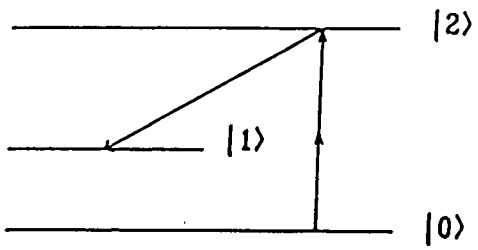

(a)

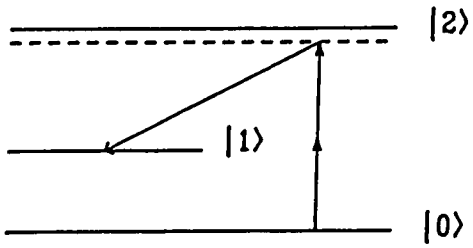

(b)

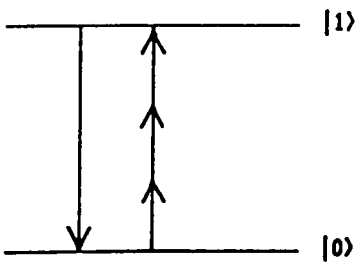

(c)

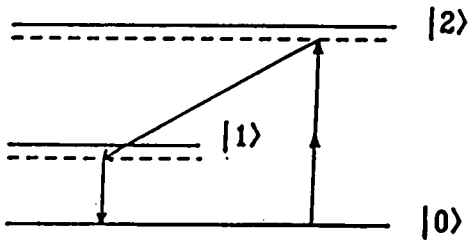

(d)

Figure 1.4. Schematic diagrams of (a) amplified spontaneous emission (ASE), (b) stimulated hyper-Raman (SHR), (c) normal four-wave mixing (FWM), (d) parametric four-wave mixing (PFWM). The dotted lines represent virtual states.

role in the experiments to be described. Instead, one of the key processes in this study is stimulated hyper-Raman (SHR) emission (see Figure 1.4b). This process involves raising the atom to a "virtual" state by the absorption of two laser photons. This leads to the production of a third photon coupling to a lower excited state ($|1\rangle$). The virtual state is defined by the energy of the two laser photons, and does not correspond to an actual atomic resonance. Unlike ASE there is no transfer of population to the intermediate virtual state prior to emission of a photon accompanied by excitation of the state in which the atom is left. This process, where the atom is left in an excited state higher in energy than the one in which it started, is often referred to as a Stokes process, and the emission is called a Stokes line. If the atom is left in a lower energy state than it was originally (this can only happen if the original state is not the ground state) the SHR emission is called an anti-Stokes line.

Since the bandwidth of the Lumonics excimer-pumped dye laser used in the present study is wider than the Doppler and collisionally broadened widths of an atomic resonance, the studies that follow can never produce a pure ASE emission. A part of the laser frequency profile is always "off resonance" due to its width, therefore, there can only be ASE and SHR combined. However, a pure SHR emission can be obtained if the laser frequency is adjusted such that the sum frequency of the two laser photons does not overlap the resonance frequency.

The last type of emission that plays a major role in the experiments to be described is four-wave mixing (FWM). Normal FWM is a process typified by the special case of third harmonic generation (see Figure 1.4c). In this process the medium absorbs three externally supplied photons whose total energy takes the atom between two atomic states (real or virtual) that have an allowed three-photon transition. These states are also coupled by a one-photon allowed transition. The medium itself generates the fourth photon back to the original state at a frequency of $3\omega_L$.

A similar, but somewhat more complicated process, is parametric FWM. In the case studied here, only two of the photons are externally supplied by the laser. The other two are generated by the medium itself (see Figure 1.4d). The atom is left in the same state in which it starts; there is no transfer of population to any intermediate state.

The index of refraction of a medium, or equivalently, the phase velocity for wave propagation through that medium, depends upon its frequency. This is called dispersion. The magnitude of the propagation vector, $|\vec{k}|$, is such that $|\vec{k}| = \omega/v$ where ω is the frequency and v is the phase velocity of the wave. If one adds up all the propagation vectors of the photons involved in a parametric FWM process, one finds that because of the dispersive properties of the medium, $|2\vec{k}_\omega| < |\vec{k}_{\omega'}| + |\vec{k}_{2\omega-\omega'}|$. In order to produce constructively interfering wavefronts, the k vectors for ω' and $2\omega-\omega'$ must adjust their angle of propagation so that phase matching can occur. That is,

the sum of the propagation vectors for the absorbed and emitted photons sum to zero (see Figure 1.5). If one lets $\vec{k}_p = 2\vec{k}_\omega - \vec{k}_{\omega'}$, represent the propagation vector for the polarization wave, phase matching can only occur when the generated wave $\vec{k}_{2\omega-\omega'} = \vec{k}_p$. If Δk is defined as the difference in magnitudes $|\vec{k}_p| - |\vec{k}_{2\omega-\omega'}|$, the phase-matching condition can be met if

$$\theta = \sqrt{\frac{\Delta k}{|\vec{k}_{\omega'}|}\left(\frac{2\omega-\omega'}{\omega}\right)} \quad .$$

and

$$\beta = \frac{\omega'\theta}{2\omega-\omega'} \qquad \text{(Payne, 1988).}$$

Since the radiation produced with frequencies ω' and $2\omega-\omega'$ is nonresonant, it is not absorbed by the medium and propagates freely out of the nonlinear medium. However, the radiation can only be generated in the forward direction (the direction of the laser photons), and will be emitted in a cone rather than along the laser beam axis. The radiation cannot be produced in the backward direction because the phase mismatch between the laser photons and generated photons would be too large, and no constructive interference could occur.

This concludes the description of the common aspects of the experiments described in detail in the following chapters. The experiments are all connected through the atomic response of sodium to a strong external electromagnetic field. Features specific to

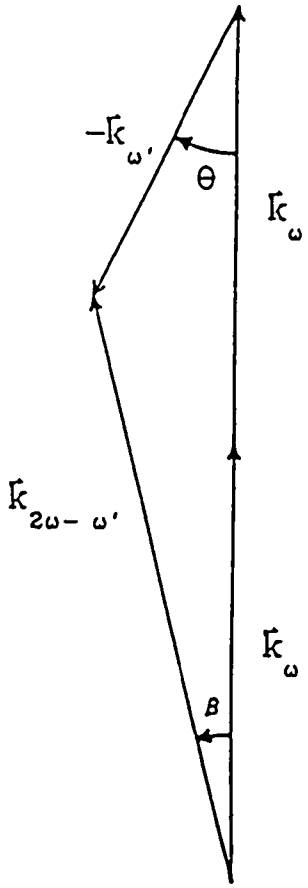

Figure 1.5. Four-wave difference mixing. The angles θ and β are determined by the phase-matching condition: $2\vec{k}_{\omega} - \vec{k}_{\omega'} = \vec{k}_{2\omega-\omega'}$.

individual experiments are described in the appropriate chapters. These include the generation and suppression of SHR emissions in Chapter II, and the effects of a.c. Stark shifts on the suppression of SHR processes and ASE in Chapter III, and conditions for axially propagating parametric FWM in Chapter IV. Chapter V consists of related phenomena which were discovered along the way that were too interesting to leave out entirely, but too narrow in scope to make an entire chapter by themselves.

The nonlinear response of a collection of "simple" sodium atoms is in fact very complex; some features are probably too complex and interwoven to entirely deconvolute experimentally. It should be emphasized, however, that sodium is not essential to the study of the nonlinear processes explored in this study, but is merely a medium in which to produce these phenomena so that their properties may be ascertained.

CHAPTER II

SUPPRESSION OF ELECTRONIC HYPER-RAMAN EMISSION BY FOUR-WAVE-MIXING INTERFERENCE

A. Theoretical Considerations

Over the past several years experimental studies (Compton et al., 1980; Glownia and Sander, 1982; Jackson and Wynne, 1982; Miller and Compton, 1982; Miller et al., 1980; Normand et al., 1983) and theoretical studies (Garrett et al., 1986; Payne et al., 1980 and 1986; Payne and Garrett, 1982 and 1983; Agarwal and Tewari, 1984) have shown that an optical interference effect may lead to the suppression of certain laser induced transitions within an atomic system at elevated number densities. More specifically, it has been shown that if an excited state may be reached by more than one optical pathway, these pathways may destructively interfere to effectively cancel the transfer of population to the atomic resonance. Theoretically it has been demonstrated that two atomic states which are coupled by any odd number of photons and are also coupled by a one-photon allowed transition may exhibit this suppression. This only occurs at pressures above a critical threshold region where the electromagnetic field responsible for the one-photon excitation process is generated in the medium itself.

One piece of experimental evidence for this effect is the suppression of resonantly enhanced ionization out of a state which is

excited by an odd number of photons (greater than one). For example, assume there exists an atomic system that is stimulated by a laser beam whose frequency is adjusted so that the absorption of four photons will ionize the atom. The probability of one atom absorbing four photons is very low. However, this process may be greatly enhanced if the laser frequency is adjusted so that the absorption of three of the photons brings the atom to a resonant state. The atom may remain in the excited state for a longer period of time, and then the absorption of a fourth photon that ionizes the atom becomes a more probable event. If certain conditions exist that suppress the resonant three-photon excitation of the atomic state, then the resonantly enhanced ionization signal will also be suppressed.

This effect has been demonstrated in xenon by Miller et al. (1980 and 1982) and Jackson and Wynne (1982 and 1983) where the presence of three-photon excitation and subsequent ionization was evident at low pressure, but suppressed at high number density. As the laser beam propagates through the moderately dense atomic medium, the suppression occurs because the electromagnetic field generated at the three-photon sum frequency (the third harmonic field explained in Chapter I under normal FWM processes) is exactly 180 degrees out of phase with the field due to three of the incident laser photons. The effect is only seen at elevated number densities because FWM processes have a minimum pressure below which the cooperative response of the atoms in the medium is too weak to offset the direct three-photon pumping of the resonance by the laser field. Because this

effect is the result of FWM, the effect may only be seen when all photons involved in the process travel in the same direction. As will be recalled from Chapter I, phase-matching considerations for the production of FWM emission demand that all photons must travel in approximately the same direction. In a situation where counter-propagating laser beams exist, the absence of a constant phase relation between fields which generate the FWM polarization prevent the generation of a FWM field and the suppression does not occur. The atom may then be excited to the three-photon resonance by the absorption of photons from both beams (i.e., at least one photon from each beam). Since no interference occurs, the expected resonantly enhanced ionization process may be observed. Several of the features of this phenomenon have been demonstrated by Garrett et al. (1986a and 1986b).

Payne and Garrett (1982 and 1983) have given a very detailed theoretical description of this cooperative interference effect which takes into account excitation with a pulsed laser of finite bandwidth, the effects of collisions between atoms, and the absorption of incident laser photons by the medium for both focused and unfocused beams. From this analysis they have predicted an additional interference phenomenon associated with stimulated hyper-Raman (SHR) scattering. As noted in the first chapter, the SHR process involves the absorption of two laser photons, to produce a third photon generated by the medium, and an atomic excitation, thereby leaving the atom in an excited state. This type of process was first named

by Decius and Rauch in 1959, and observed for the first time by Terhune et al. in 1965 in molecular species. Vrehen and Hikspoor (1977) were the first to see an electronic SHR process involving an atomic transition in a gas. This process can be greatly enhanced if the laser frequency, ω_L, is such that $2\omega_L$ is near a two-photon allowed resonance in the medium.

As was illustrated above, the three-photon resonance cancellation by interference with an allowed one-photon resonant emission is theoretically well established and supported by much experimental evidence (see also Garrett et al., 1986; Miller and Compton, 1982; Miller et al., 1980; Orlando et al., 1986; Payne et al., 1980). The suppression mechanism has its onset at very low pressures, and it is independent of the laser field intensity. A new prediction which forms the basis of the study for this chapter is that this interference effect also affects the forward SHR emission. In effect, the SHR emission which is a three-photon process to a resonance is exactly 180 degrees out of phase with a FWM emission that is generated by transitions between the 3p or 4p states to the ground state. This 180 degree phase difference between two pumping mechanisms (in the forward direction) effectively destroys any forward SHR production (Moore et al., 1988) while leaving the backward propagating SHR unaffected. It is predicted that the effect occurs when $\Gamma < 2\pi Nz|D_{01}|/\hbar c$, where N is the number density, z is the distance traveled into the nonlinear medium, $|D_{01}|$ is the matrix element between the connected states, Γ is the bandwidth of the laser, $\hbar$ is Planck's constant, and c is the speed of light in vacuum (Payne et al., 1986). At a number density equivalent to one torr of sodium vapor, z is less than one cm in the following experiments.

The phase-matching considerations for parametric FWM processes are described in Chapter I. Since the phase-matching conditions necessary for FWM in a pure vapor can only occur by adjusting the angles of the propagation vectors of the generated waves, the FWM photons will not travel down the axis of the pump laser beam (exceptions to this rule have been discovered which form the basis for Chapter IV). As discussed in Chapter I, SHR emission results from an exact three-photon resonance excitation. It travels along the laser axis because it is the result of a stimulated process that has a higher probability of occurring in directions that keep the stimulating photons within the laser field. Therefore, the SHR and FWM signals may be separated by geometrical propagation considerations. Since the waves each have k vectors of different lengths, wavelength discrimination is also a viable technique for distinguishing one process from another with a spectrometer of sufficient resolving power. The experiments described in the next section explore the SHR phenomenon and demonstrate that SHR emission is indeed suppressed in the direction of the laser photons, resulting in a unidirectional backward SHR emission.

B. The Experiment

In this study, ground state sodium atoms are pumped near a two-photon resonant d state, with total angular momentum quantum numbers either $j = 3/2$ or $j = 5/2$. Since the sodium nucleus has an odd number of nucleons (11 protons and 12 neutrons), a hyperfine splitting also occurs from the interaction of the nuclear spin with the spin of the single electron in the valence shell. However, this splitting is

extremely small, and does not play a role in the experiments that follow. An internally generated photon is produced by a resonant SHR process from near the d states to a 3p state (either j = 1/2 or j = 3/2). The fourth wave in the FWM process is produced by photons generated from either of the 3p states to the 3s ground state (see Figures 2.1a and 2.1b).

When the incident laser is tuned exactly to the two-photon resonance with a d state, the emission process changes character because energy can now be stored in the atomic d states. Amplified spontaneous emission (ASE) replaces the SHR mechanism, and the ASE photons may propagate in either the forward or backward direction.

As already mentioned, two-photon pumping near d states in sodium also produces parametric four-wave difference mixing emission. The production of phase-matched conically emitted FWM emission for transitions from the 3p to the 3s states has been well documented by Krasinski et al. (1985). This study is not concerned with this conical emission, but rather with light that is emitted parallel or antiparallel to the incident laser beam, the SHR emission.

A heat pipe was operated with sodium vapor at a pressure of about two torr and excited by a Lumonics excimer-pumped dye laser tuned to the two-photon resonance with either the 3d or 4d state. The bandwidth of the laser (0.04 cm^{-1}) is insufficient to resolve the d state fine structure levels. Although the interference process under consideration here is independent of laser energy, the data presented involved the use of laser power densities of $\sim$7.0 MW/cm^2 for the 3d case and $\sim$30 MW/cm^2 for the 4d case.

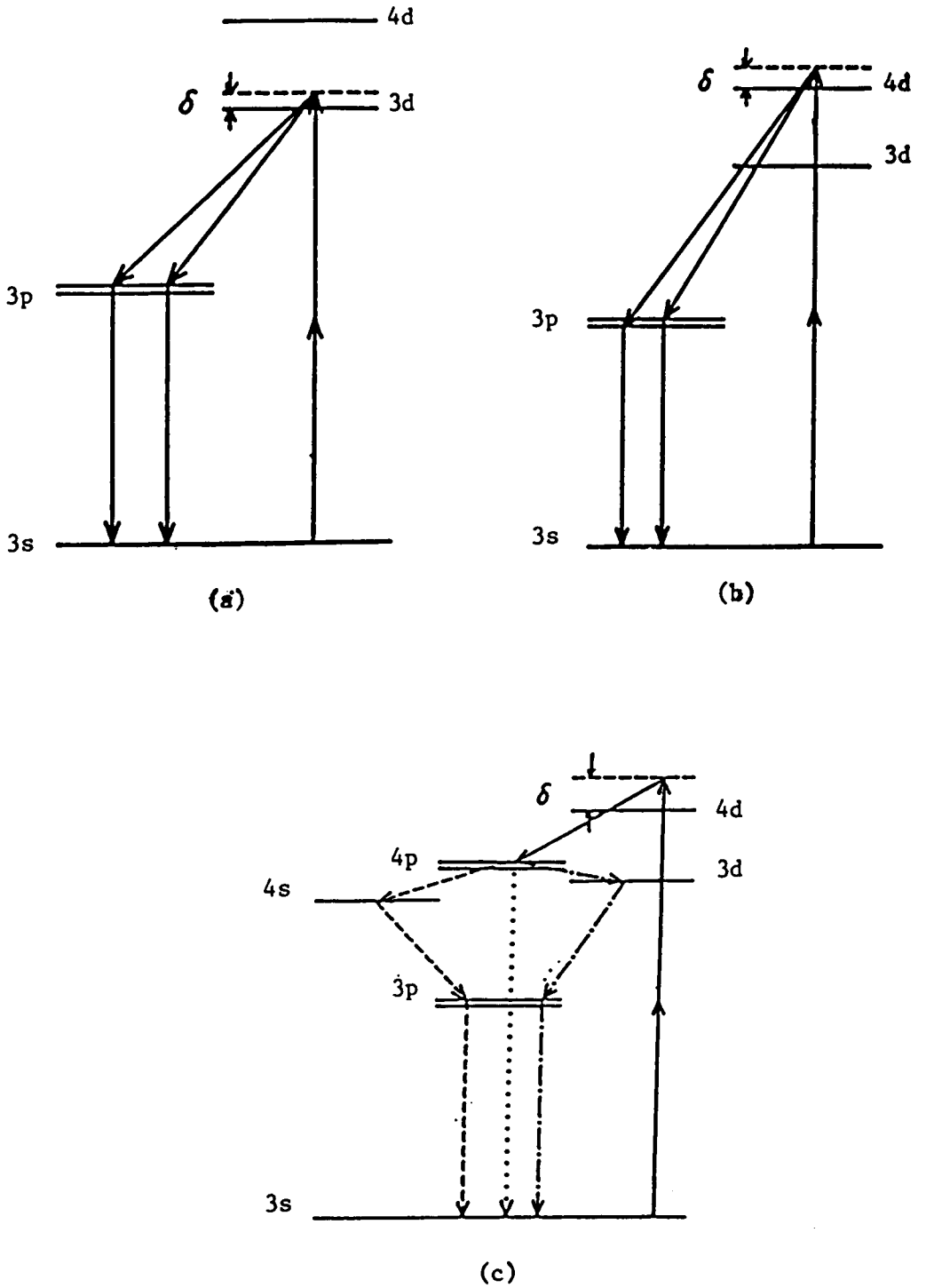

Figure 2.1. Schematic of two-photon processes in sodium, SHR from (a) 3d, (b) 4d states, (c) alternate routes out of 4d states. δ is the detuning of the incident laser from the two-photon resonance.

Light from the 3d-3p transitions at 8194 Å and 8183 Å for transitions to the $3p_{3/2}$ and $3p_{1/2}$ states, respectively, were analyzed by a Jarrell-Ash spectrometer in both the forward and backward directions. The incident laser was tuned off resonance and the beams analyzed again. A similar technique was used to analyze the $4d\text{-}3p_{1/2,3/2}$ photons that have λ = 5684 Å and 5690 Å, respectively.

In each case the laser beam was reduced to a 0.3 cm diameter by the use of apertures before entering the heat pipe to produce a spatial beam profile that was Gaussian shaped in a direction perpendicular to the propagation of the laser photons. A 0.5 cm aperture was placed in the forward beam after it had exited the heat pipe to discriminate against the conical FWM emission expected in that direction. Since the spectrometer used had a resolution of 0.3 Å at best, discrimination of SHR emission and FWM signals by wavelength was not practical. In the 4d case a 50-cm focal length lens was used to focus the laser beam into the center of the heat pipe. This pipe has a sodium vapor length of approximately 28 cm. A higher energy density was necessary in the 4d case due to the additional competing paths for the transitions back to the ground state not available in the 3d case (see Figure 2.1c).

Special care was taken to insure that collection techniques for both forward and backward beams were matched so as not to favor either beam. Both were collected by glass wedges (or matching mirrors in the 4d case) that reflected $\sim$4% per surface reflection. Guiding the respective beams into the spectrometer was accomplished by rotating a

99% reflecting aluminum mirror to intercept only one reflection from either beam. The path length between the heat pipe center and the spectrometer differed at maximum by only 4 cm (see Figure 2.2). Spectral data scans were alternated between directions keeping the laser frequency fixed, to assure both beams were compared at exactly the same laser frequency. Results are shown in Figures 2.3 and 2.4. Notice in the 3d case (Figure 2.3a) that when the laser is tuned exactly to the two-photon resonance the backward beam intensity is greater than that of the forward beam. Since the laser is tuned to the 3d resonance this emission has an ASE component as well as a contribution from the SHR process. The ASE portion of the signals is not affected by the specific suppression effect mentioned earlier, but it may be affected by another interference phenomenon that will be covered in the next chapter. In Figure 2.3b the laser is now detuned by 0.1 Å to the high energy side of the 3d resonance. The forward beam intensity (now pure SHR since the detuning is greater than the bandwidth of the laser) is drastically reduced while the backward beam intensity remains almost the same as at zero detuning. When the laser is further detuned from resonance by 0.2 Å (high energy side, Figure 2.3c), the forward SHR signal is completely suppressed, while the backward SHR emission, although weaker, is still strongly in evidence.

If there were no suppression effect on the forward SHR emission, the backward and forward emissions should be identical.

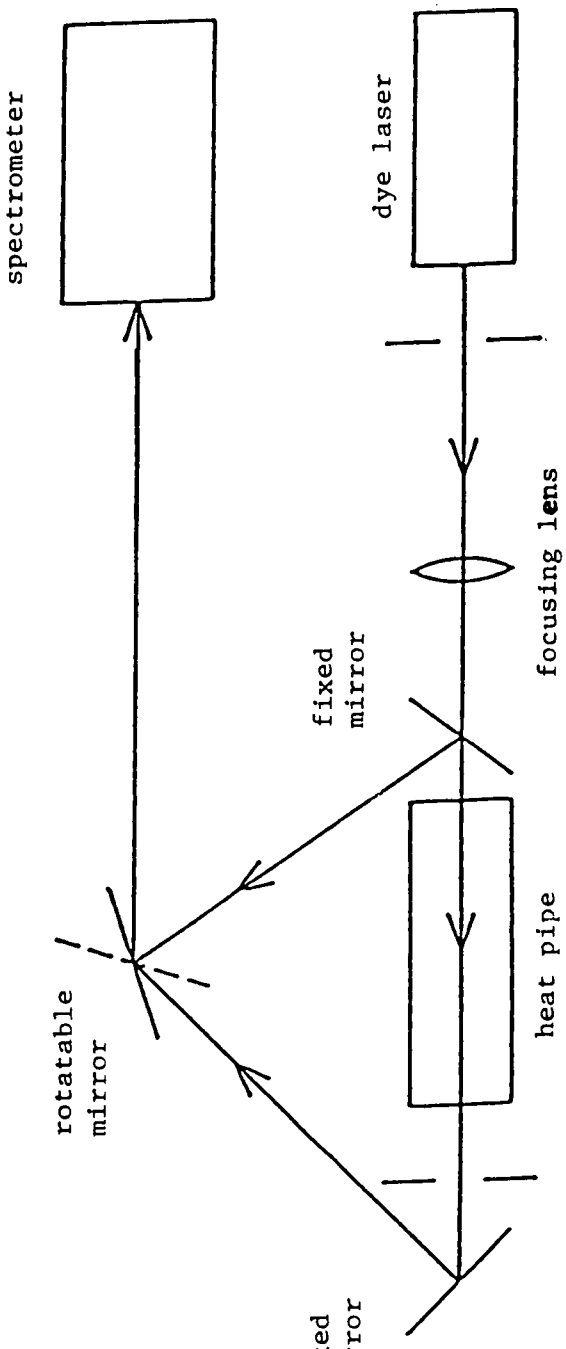

Figure 2.2. Schematic diagram of experimental setup for demonstration of suppression of forward SHR.

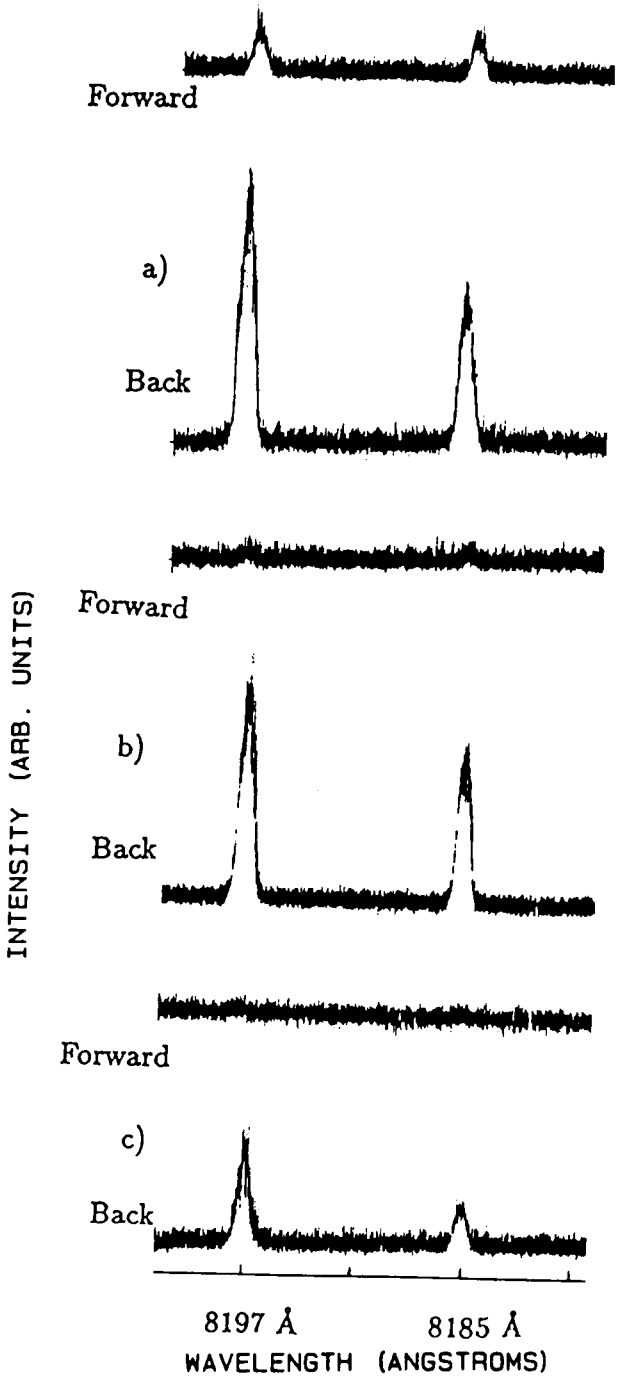

Figure 2.3. Spectral scans of SHR from 3d states at various detunings: (a) 0 Å, (b) 0.1 Å, (c) 0.2 Å, P = 1.5 torr, I = 7.0 MW/cm^2, 8185 Å = 3d-3p$_{1/2}$, 8197 Å = 3d-3p$_{3/2}$, predicted threshold for this process is 7 x 10^{-5} torr of sodium (Moore, 1988).

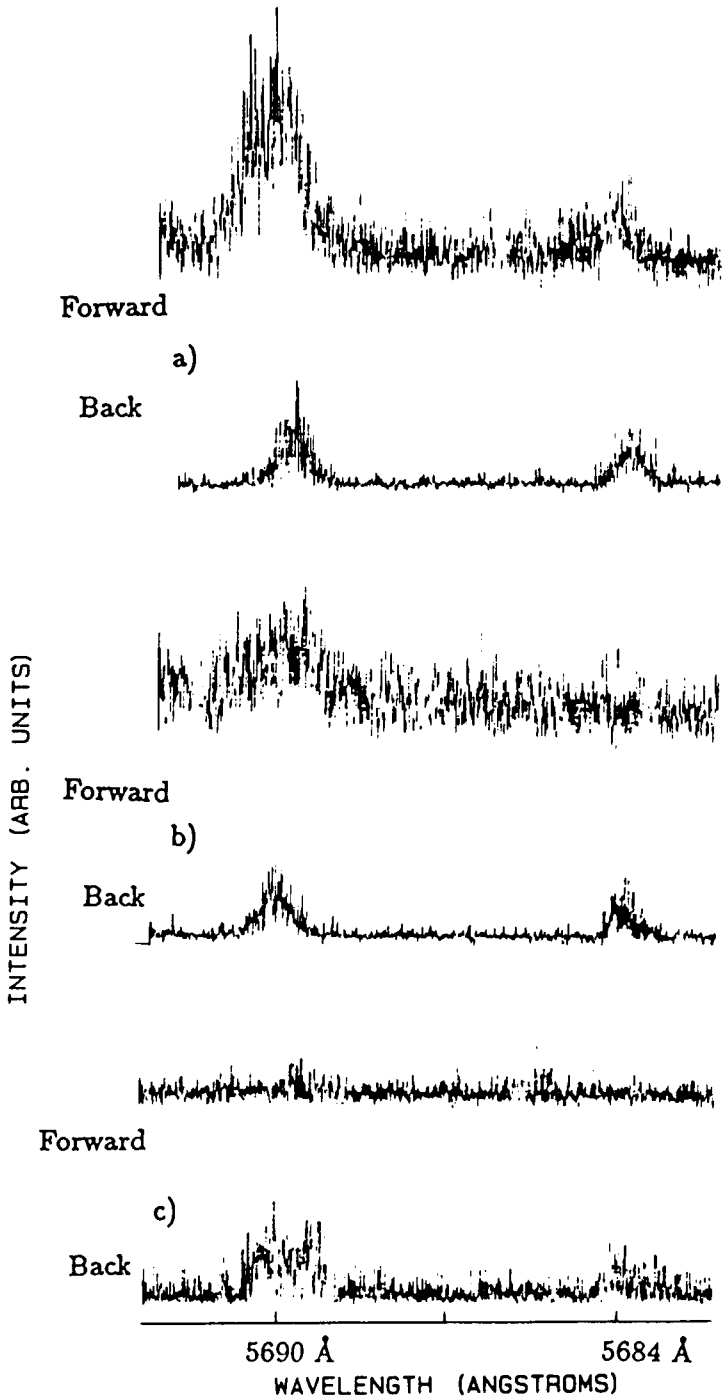

Figure 2.4. Spectral scans of SHR from the 4d state at various detunings: (a) 0 Å, (b) 0.1 Å, (c) 0.3 Å, P = 1.5 torr, I = 30 MW/cm^2, 5684 Å = 4d-3p$_{1/2}$, 5690 Å = 4d-3p$_{3/2}$, predicted threshold for this process is 7 x 10^{-5} torr of sodium (Moore, 1988).

Since the forward signal is drastically reduced compared to the backward one, a strong suppression effect is clearly in evidence as predicted by Moore et al. (1988).

The 4d case presented in Figure 2.4 shows a similar behavior. However, at zero detuning (Figure 2.4a) the forward beam intensity is now greater than the backward intensity. This is due to the fact that although it is possible to pump the 4d resonance more efficiently because of the higher laser energies available at this frequency, the transition probability between the 4d and 3p states is much lower than that between the 3d and 3p states. At a detuning of δ = 0.1 Å to the high energy side (Figure 2.4b), the axial signal is pure SHR emission and the signal in the forward direction is greatly reduced. When the laser is tuned 0.3 Å to the high energy side of the resonance (Figure 2.4c) the forward SHR emission is completely suppressed. The amplifier gain for Figure 2.4c is slightly higher than that for Figures 2.4a and 2.4b.

To reiterate, although there are differences in the SHR emission intensities when pumping to either the 3d or 4d resonances, there is clear evidence for the suppression of the forward SHR emission as compared to the backward propagating signal. In both cases, SHR emission to the 3p state is drastically reduced in the forward direction while the backward SHR signal behaves as expected.

Observation of emissions associated with pumping near the sodium 4d state presents several experimental difficulties; the first is the weakness of the signal. When one examines the energy level

diagram of sodium up to the 4d state (see Figure 2.1c) one can see that there are at least three more favorable routes from the 4d state to the 3s ground state. These paths all go through the 4p states and their more favorable nature can be seen by examining the oscillator strengths between available states (see Table 1.1, p. 10). Since the SHR emission resulting from a transition from near the 4d states to the 3p states is weak, it is necessary to enhance the signal by increasing the voltage on the photomultiplier tube, which results, of course, in a much noisier signal.

In addition there is another forward emission in the 4d-3p frequency range that makes data recording difficult. If one lets the entire forward beam (cone and axial parts) into the spectrometer, one sees a very large broad band emission upon which the atomic peaks are superimposed. This broad band emission covers several dozen angstroms and is not evident at all in the 3d-3p case. This band seems to change shape and location as a function of laser intensity, and does not exist in the backward direction. Furthermore, it is eliminated when the forward aperture is in place. This implies that the light is not axial in nature and, therefore, not part of some stimulated process. Dimer emission may be eliminated from the possibilities because dimers make up at most only a few percent of the beam at these pressures (Gordon et al., 1971). In addition, the location of their emissions should not be affected by laser intensity. It is possible, however, that what is being seen is fluorescent emission from the laser dye itself. The shape and width of the

emission band (about 60 Å) is in the correct region for the dye used in this experiment (Rhodamine 590).

Additional evidence for the cancellation effect involving forward SHR emission has also been found by scanning the dye laser across either the 3d or 4d two-photon resonances and observing the axial emission in the backward and forward directions. The data presented in Figure 2.5a show axial emissions resulting from the two-photon pumping of the 3d states with emission in the λ = 8197 Å range. Figure 2.5b has the axial emission from the two-photon pumping of the 4d states. However, instead of emission from the 4d-3p states as presented earlier, this is emission from another three-photon SHR process. This emission results from transitions coupled to the 4p rather than the 3p states. Here the wavelength is approximately 23,300 Å. It is easily seen that the forward emission is narrower in range than the backward emission in both cases (see Figure 2.5). This is further evidence that the SHR emission in the forward direction is suppressed, since the SHR process, if not interfered with, should have the same line profile in either direction.

When one studies the SHR emission from the 4d-4p transition in the same manner that was done for the 4d-3p and 3d-3p transitions (i.e., keeping the laser frequency fixed and scanning the SHR emission with a monochromator) no suppression of axial emission in the forward direction is seen. This may be explained by the fact that another type of axial emission has been discovered. As will be

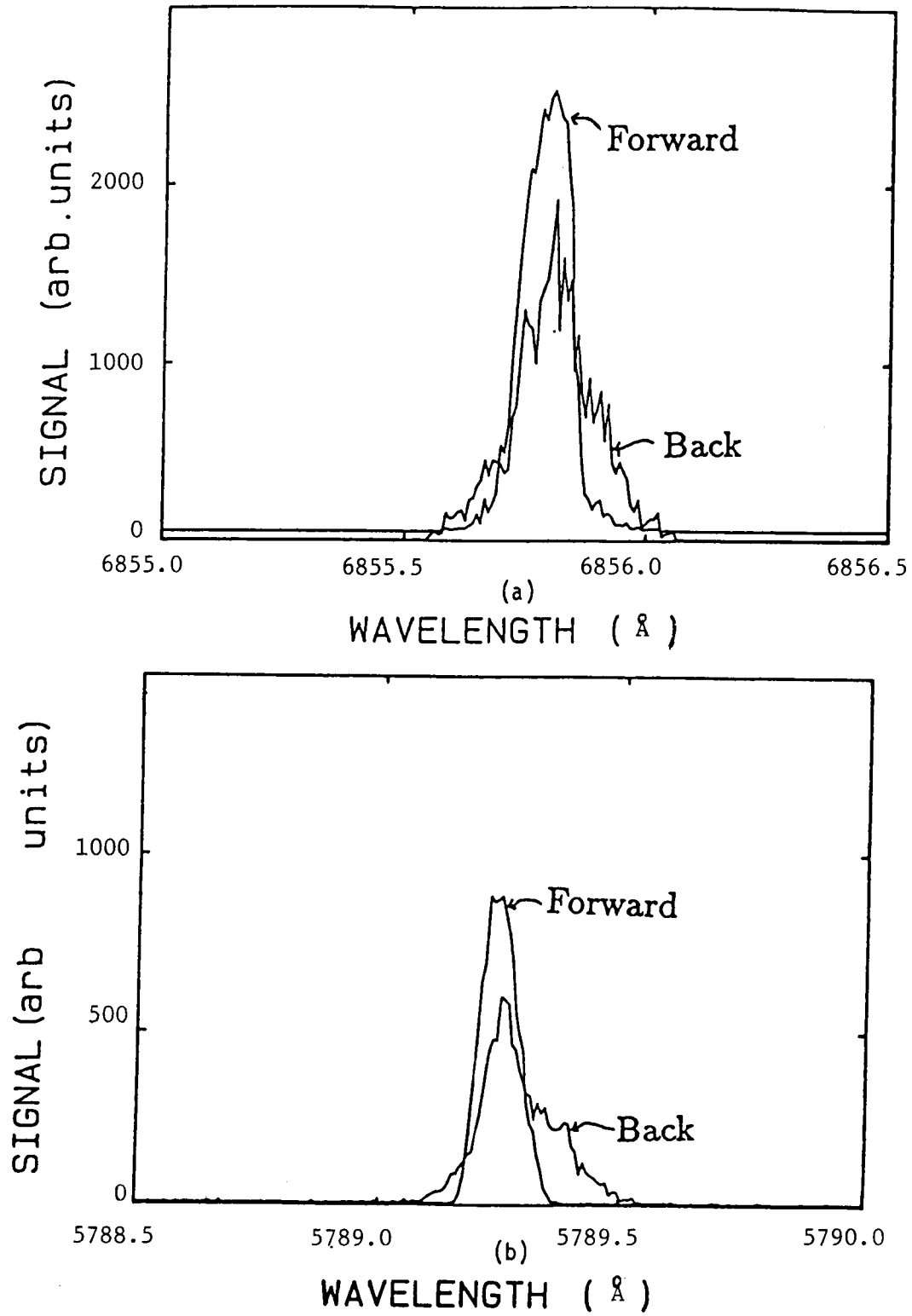

Figure 2.5. Backward and forward axial emissions while tuning the laser across two-photon resonance. (a) 3d resonance, P = 2.5 torr, E = 2 mJ/pulse, $\lambda \simeq 8200$ Å; (b) 4d resonance, P = 0.02 torr, E = 3.5 mJ/pulse, $\lambda \simeq 23{,}300$ Å.

explained further in Chapter IV, there exists another process that propagates axially, but is neither ASE or SHR emission. Under certain circumstances, there is an axially produced PFWM emission. With the limited resolution available in the 4d-4p frequency range (λ=23,300 Å), it can be shown that in all probability the axial emission seen in this frequency region in the forward direction is in fact FWM emission rather than SHR. The evidence consists of spectral scans of the axial emissions in both forward and backward directions in the 23,300 Å range. As can be seen in Figure 2.6, the separation between transitions to the two fine structure peaks ($4d\text{-}4p_{3/2}$ and $4d\text{-}4p_{1/2}$) is wider in the forward direction. Since the backward emission can only result from ASE or SHR processes this splitting must match the separation of the levels (5 cm^{-1}). The increase in forward splitting can only be due to a process that shifts the frequency from exact resonance such as a FWM process.

C. Conclusions

A suppression effect is clearly evident when a SHR process leads to the three-photon excitation of a state that is also coupled to the ground state by a one-photon transition. However, SHR processes may also be suppressed (less dramatically) by competing processes. This study is closely allied to a two-color experiment reported by Garrett et al. (1986), except that the third photon is generated by the medium itself rather than being supplied externally

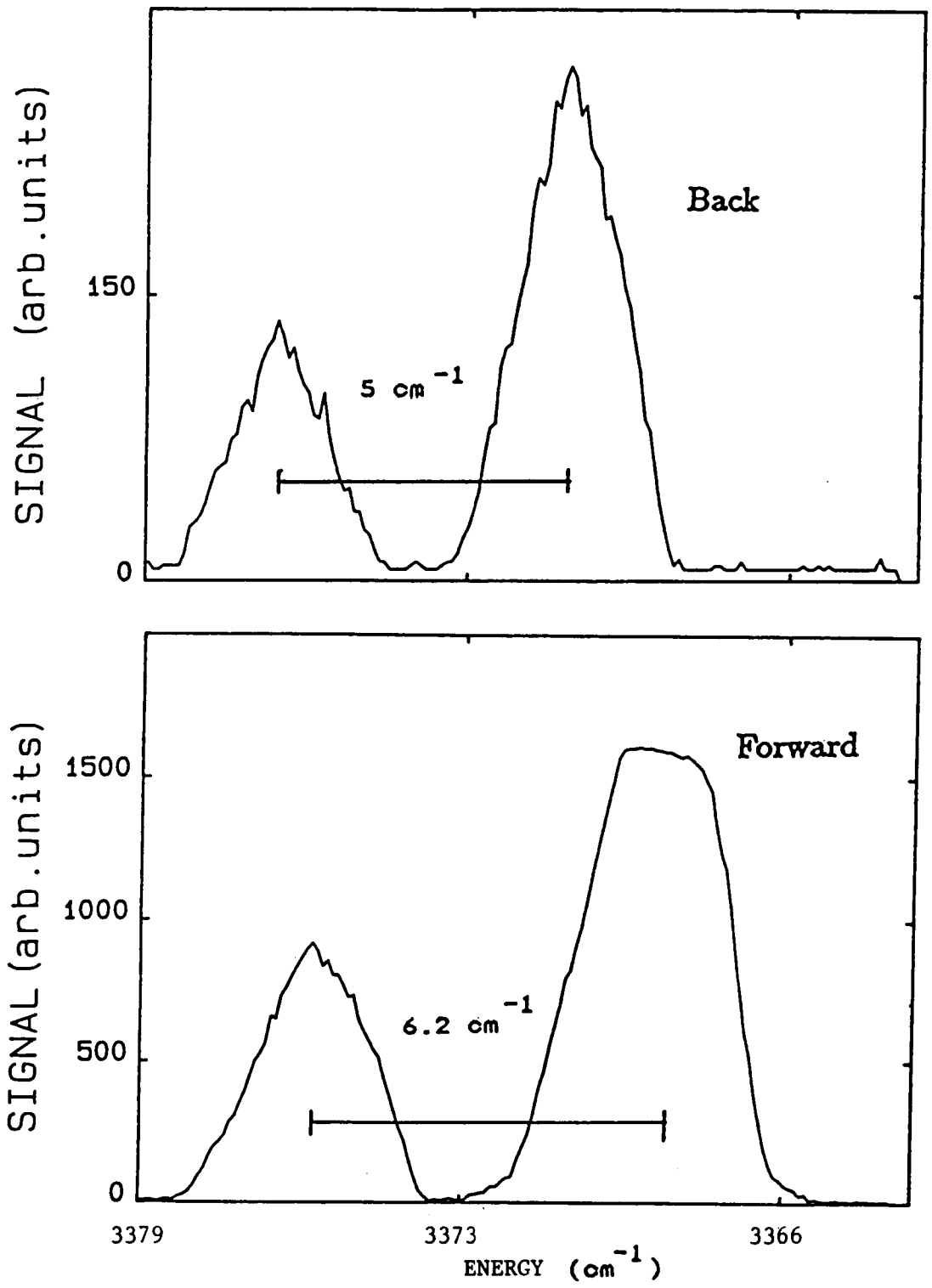

Figure 2.6. Spectral scans of forward and back axial emission in the 4d-4p frequency range. $\lambda \simeq 23{,}300$ Å when the laser is fixed on the two-photon 4d resonance, P = 2.0 torr, E = 2.1 mJ/pulse.

by another laser. Other interesting phenomena were discovered while doing this study and they will be discussed in the next chapter.

CHAPTER III

THE SUPPRESSION OF TWO-PHOTON PUMPING OF SODIUM RESONANCES

Suppression of multiphoton processes due to competition with other nonlinear phenomena has been an avid topic of interest in the field of nonlinear optics over the past several years both from a theoretical and an experimental standpoint. The suppression of resonantly enhanced ionization due to cancellation of the three-photon resonance by a four-wave mixing interference as discussed in Chapter II is a case in point (for other examples see Agarwal et al., 1984; Ashfold et al., 1986; Garrett et al., 1986; Jackson and Wynne, 1982; Jackson et al., 1983; Boyd et al., 1987; Payne et al., 1982 and 1986). Interesting observations have been made in several studies that have shown how certain nonlinear processes in extended media can interfere with the expected intensity rates of other resonant multiphoton processes. Some of these observations are noted in the following section.

A. Observations

In Chapter II it was shown how an odd-photon transition that is also coupled by a one-photon transition can be cancelled due to destructive interference between two pathways when the extended nonlinear medium has sufficiently high number density. This was

shown by the suppression of forward stimulated hyper-Raman (SHR) emission, a three-photon resonance process.

Various phenomena have also been observed involving the pumping of a two-photon resonance. These observations include: (1) the suppression of ASE when pumping to the two-photon 3d resonance, (2) a saturation effect in the production of backward SHR when pumping the system at high laser power densities, and (3) the weak absorption of laser photons when two counterpropagating beams are propagated through the absorbing medium.

The suppression of ASE under conditions of high power density laser pumping in sodium vapor was reported by Malcuitt et al. in 1985. In their experiment they pumped an atomic sodium system at a pressure of 1.5 torr to the two-photon 3d resonance and measured the ratio of backward to forward emission from the 3d to 3p states as a function of laser intensity. The forward emission contained radiation from both ASE and FWM processes, while the backward beam was pure ASE due to the phase-matching constraints on FWM emission. They found that this ratio decreased as the laser power density increased. This observation indicates that ASE production is reduced as compared to FWM as the intensity of the laser pumping is increased even though ASE production is more efficient by a factor of 100 as compared to FWM (Malcuitt et al., 1985). These investigators proposed that the FWM emission suppressed the ASE production through an interference effect involving the simultaneous coupling of a two-photon resonance by two laser photons and two photons that are generated in the medium

by PFWM. Boyd et al. (1986) have given a theoretical basis for the FWM interference effect that suppresses ASE production from a two-photon excited state. The study by Boyd et al. was presented as an extension of the multiphoton interference effect in xenon discovered at Oak Ridge National Laboratory, and discussed in Chapter II. Of equal interest was the fact that an interference between two-photon pumping and an internally generated PFWM process was predicted theoretically by Manykin et al. (1965) more than twenty years ago, but was not observed experimentally until the claim by Malcuitt et al. in 1985.

However, doubt was cast over these conclusions following further experiments done in the present study. If the interference effect suggested by Boyd et al. was responsible for the observed suppression then other predictable behavior should also be observable. First, there should be an increase in the absorption of the laser beam through the medium when two laser beams are counterpropagated through the vapor region. Under this condition the four-wave mixing process is suppressed because of the phase mismatch that results when a photon is absorbed from each counterpropagating beam. Second, ionization signals should show a dramatic increase when counter-propagating laser beams are spatially and temporally overlapped. As was explained in the last chapter, this is also due to the suppression of four-wave mixing processes that prevent an atom from remaining in an excited state. Electrons are now more easily promoted to higher

states where they may be easily ionized by either another laser photon or a photon generated in the medium.

Experiments were devised to test for both of these expected fingerprints of Boyd's purported interference phenomena and the corroborative evidence was not found. The laser absorption experiment was conducted as follows. By using a beam splitter, counter-propagating beams were sent through the sodium vapor so that they overlapped temporally in the center of the heat pipe vapor zone. Mirrors directing the beams into either end of the heat pipe could be adjusted so that the beams could be overlapped spatially as well. The laser was tuned over both the two-photon 3d and 4d resonances and the absorption profile of one of the beams was monitored by a photodiode. Each beam individually produces a FWM signal as it propagates through the sodium vapor, and this signal may interfere with pumping the two-photon resonance. However, when the beams are counterpropagated another mechanism is present for pumping the two-photon resonance that does not produce a FWM signal. This occurs when one photon is absorbed from each beam, and the phase mismatch between the laser photons prevents the production of FWM. It is the excitation and subsequent ASE produced by this mechanism that would account for the enhanced increase in laser absorption if one were to occur.

When the beams were overlapped both spatially and temporally, four-wave mixing was suppressed due to the phase mismatch of one photon coming from either beam, and there should be a dramatic

increase in laser absorption due to other processes such as ASE and SHR emission that do not depend on phase-matching considerations. As can be seen in Figure 3.1, there is no significant increase in either case. In the 3d case virtually no increase in absorption was found. In the 4d case a small, but insignificant, increase is observed when the beams are counterpropagated.

Another piece of evidence for Boyd's interference effect, at least in principle, would be an increase of ionization when the counterpropagating beams are overlapped. As explained earlier, if more two-photon excitation occurs, thereby transferring a greater population to higher states, there should also be an increase in resonance enhanced ionization. A set of experiments were performed to reveal the ionization behavior. However, there are many problems associated with an ionization measurement technique when applied to resonance phenomena. Figure 3.2 shows plots of ionization signals when copropagating and counterpropagating two laser beams of different frequencies. One laser was kept at a fixed frequency approximately ten angstroms to the high energy side of the resonance, while the other laser was scanned in a manner such that the peak on the left is due to two photons from the nonfixed beam scanning across the 3d resonance frequency while the peak on the right is due to one photon from each beam summing to this resonance frequency. In Figure 3.2, the plots of backward SHR emission underneath (marked IR because they are in the infrared portion of the frequency spectrum at $\lambda \simeq 8197$ Å) give confirmation as to where the resonances occur. If

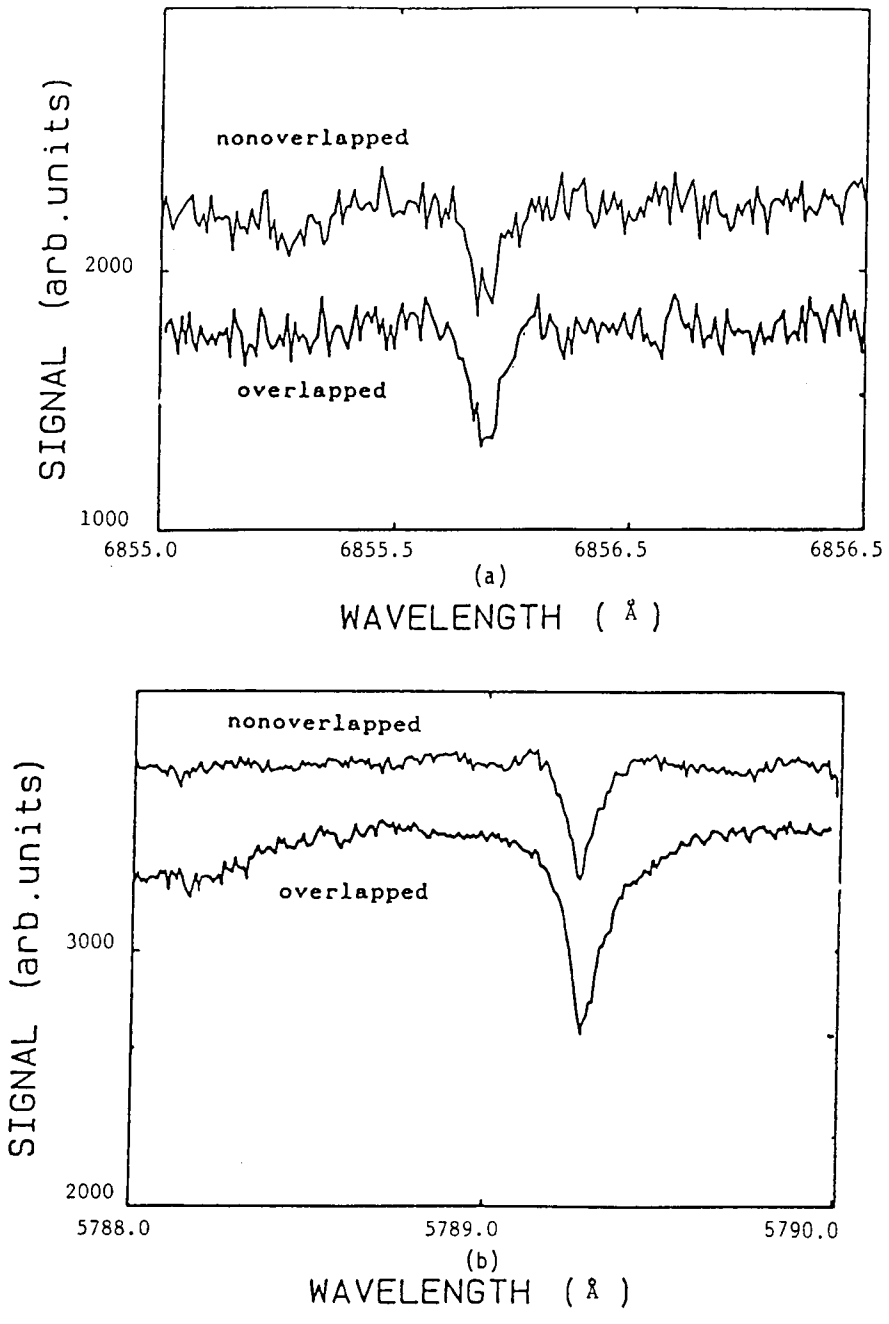

Figure 3.1. Laser absorption profiles for overlapped and nonoverlapped beams when laser is tuned across the two-photon (a) 3d, (b) 4d resonance. No significant increase in absorption is seen in either case.

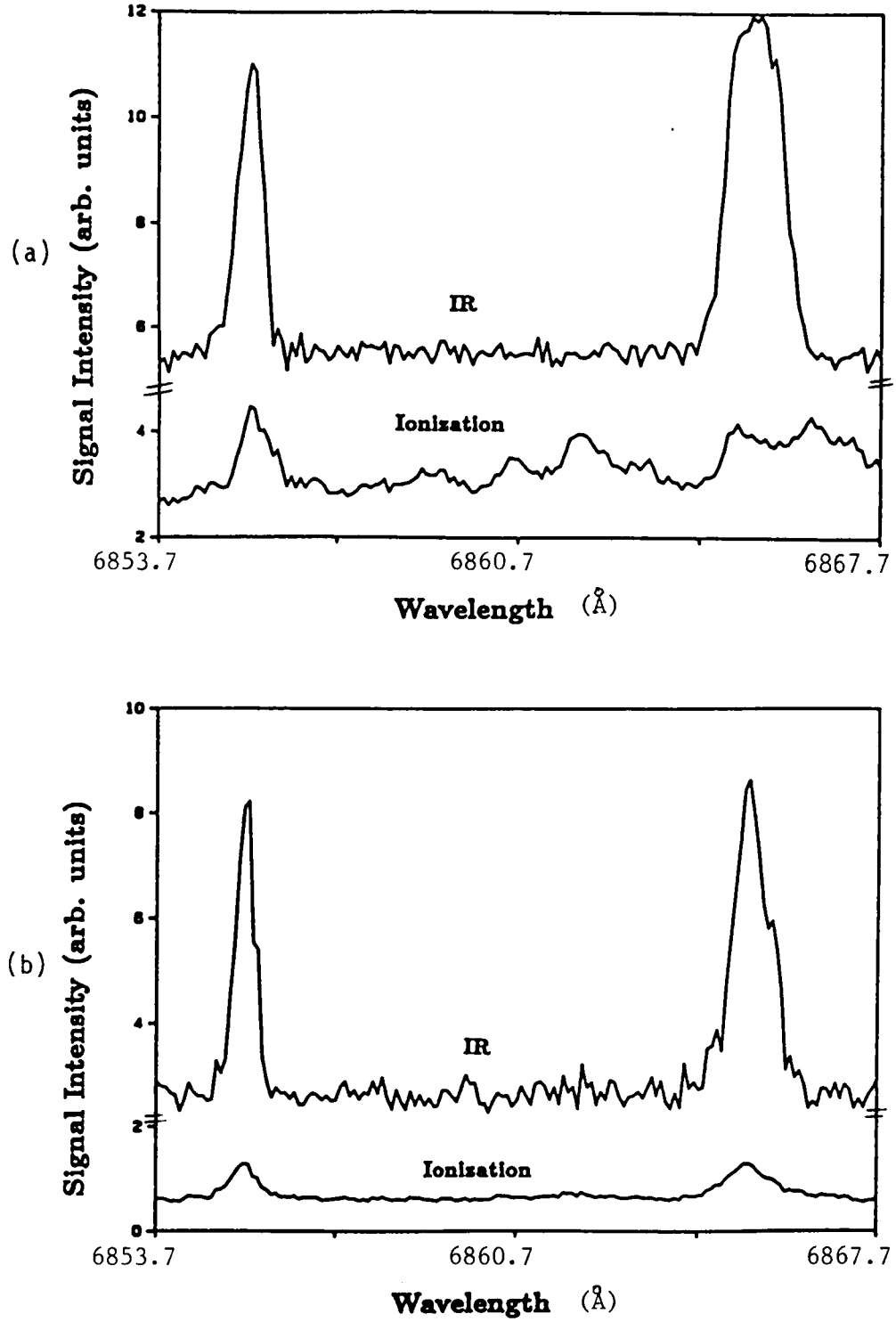

Figure 3.2. Ionization and SHR signal (labeled IR) while (a) counter- and (b) copropagating two lasers of different frequencies. P = .005 torr, E = 2 mJ/pulse. Signals are plotted on the same intensity scale.

one examines these data it seems quite evident that there is no increase in ionization in the counterpropagating beam case. There, in fact, appears to be a decrease. Therefore, with counterpropagating beams there is no increase in population transfer and, hence, no increase in ASE according to these data.

However, this apparent lack of increased ionization when counterpropagating the laser beams is not a true indication of the degree of ionization of the sodium vapor. This was discovered while carrying out further experiments involving ionization measurements. The well-known phenomenon called space charge can limit the ability to measure true ionization yields when there are a great many ions present (McDaniel, 1964). In the present heat pipe studies a positively biased wire was used to collect electrons to measure ionization. If something prevents these electrons from reaching the wire (for instance, electrostatic attraction by a line of positive sodium ions, of which there are a great many), then the ionization signal associated with the collection of photoelectrons is anomalously low even when the degree of ionization is quite high.

There also exist other processes which may cause ionization yields to be low. These include recombination, electron attachment, and radiative attachment. Recombination can only occur if space charge exists initially. Since the electrons are being pulled away from the ionization region by applied voltage on the collection wire, there is only a small probability of this process dominating the space charge effect. Electron attachment is a three-body problem that does not play a significant role in these experiments due to the

rather low number densities of atoms involved. Radiative attachment consists of the following process:

$$e^- + Na \rightarrow Na^- + h\nu \ .$$

It is another process of very low probability. The point to be made is not which process thwarts the measurement of ionization yields, but rather that many processes exist that may lead to spurious measurements of ionization signals.

It should be emphasized, however, that ionization measurements of this type are perfectly reliable at very low densities and away from resonances where little ionization occurs. However, in the pressure and laser intensity regions necessary to see the ASE suppression, which also requires being on resonance, the measurements are found to be unreliable. This was found to be the case whether pulsed or dc electronics were used to measure the ionization signals.

Thus, even while ionization measurements are not conclusive, the lack of increase in laser beam absorption when counterpropagating two laser beams indicates that FWM is not the mechanism that suppresses ASE, as claimed by previous investigators (Boyd et al., 1987).

The second two-photon resonance phenomenon listed earlier was the saturation of the backward SHR emission when pumping the system at high laser intensity. As seen in Figure 3.3, the backward SHR signal only increases linearly as a function of laser intensity after a threshold laser energy is reached. A normal SHR emission would

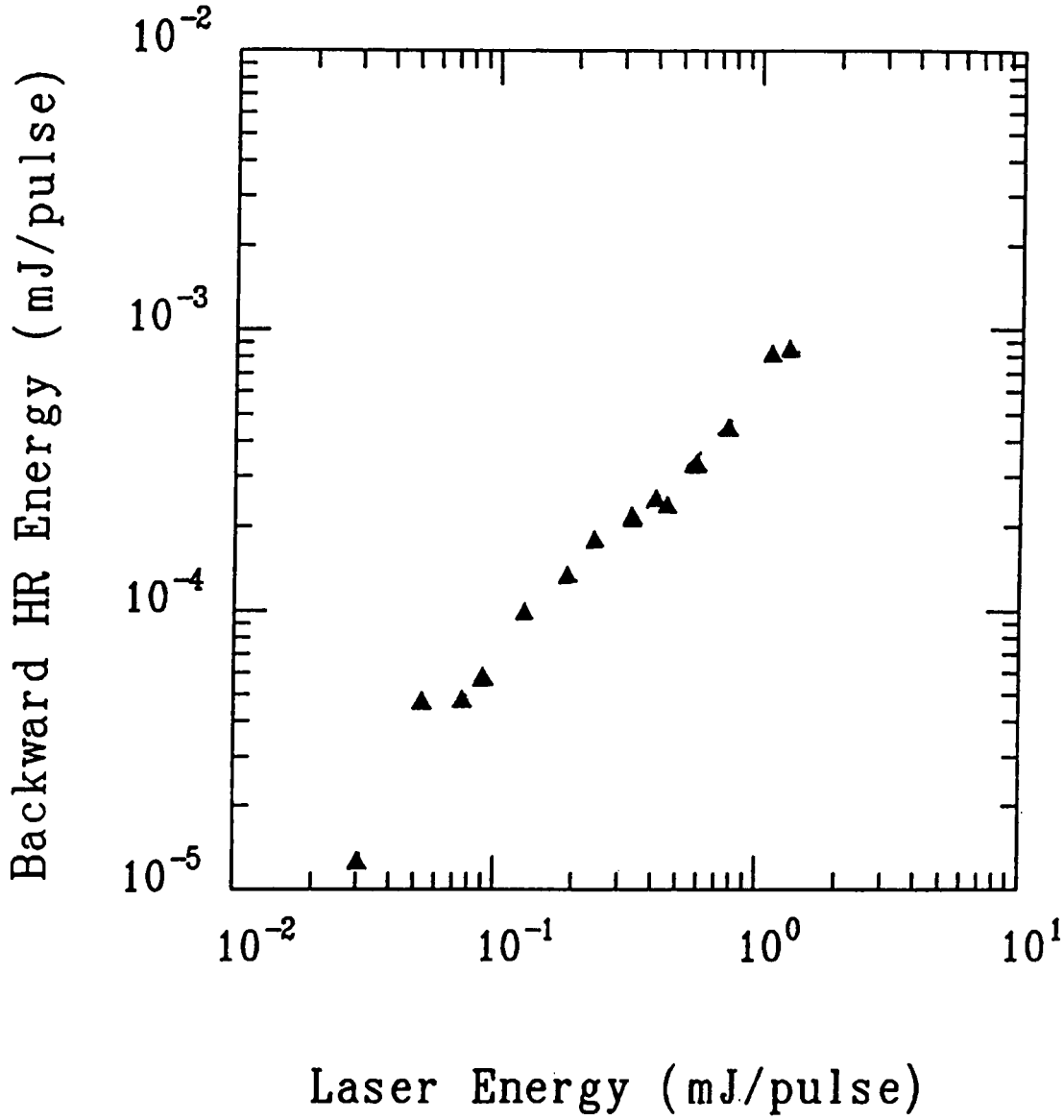

Figure 3.3. Absolute energy values of backward IR hyper-Raman emission as a function of incident laser intensity at low sodium vapor pressure, P = 0.07 torr. Energy values were measured with a Scientech 362 power energy meter with a rated accuracy of ±3%.

increase quadratically (Hanna, 1979). Payne et al. (1988) have a theoretical model that explains why the SHR emission changes from a quadratic to linear function of the laser field that is based on the a.c. Stark effect.

The next section deals with experiments that endeavor to provide an understanding of the suppression of phenomena that originate with a two-photon pumping process. This includes both the suppression of ASE and the saturation of backward SHR emission as a function of laser intensity.

B. The A.C. Stark Effect

From the analysis in Chapter II, it is evident that above a threshold pressure regime (the absolute value of which is dependent on the one-photon oscillator strength of the relevant transition, Moore, 1988), no forward SHR emission can exist under circumstances where the associated atomic resonance can be reached by both three photons and a single photon. However, backward propagating SHR photons can still be generated in the medium. Observations have shown (Figure 3.2) that there is also a mechanism in addition to the interference effect that limits the backward SHR intensity as a function of laser intensity.

On the basis of this study the mechanism that can explain both the suppression of backward SHR emission and the suppression of ASE observed by both Malcuitt and her associates and in the present work can be shown to be the dramatic influence of the a.c. Stark

effect on resonant two-photon excitation in dense media. The a.c. Stark effect causes the shifting of atomic levels, most significantly by near-resonant light. As will be shown below, dramatic a.c. Stark shifting is produced not by the laser field itself, but by the internally generated fields. Although these fields are weaker than the one produced by the laser, they produce near-resonant coupling between the levels of concern, and lead ultimately to a large suppression of the two-photon mediated process.

The magnitude of the a.c. Stark shift may be calculated from the expression for the Rabi frequency between two given states if the power density of the coupling radiation is known (Hurst and Payne, 1988). Two sources of radiation exist that contribute to the magnitude of the Stark shifting of the 3d state. The first is the laser beam that connects the 3s and 3d states. The second is the ASE and SHR emission that couples the 3p states to the 3d states.

The frequency of the laser beam is far from any resonant frequency of the sodium atomic system. When pumping with far off-resonant light the magnitude of the a.c. Stark effect depends quadratically on the field strength. For transitions between the 3s ground state and the 3d state it has the form (Bakos, 1977):

$$\Delta_s = \frac{E^2}{2\hbar^2} \sum_{\beta} \left\{ \frac{\langle 3s|\hat{D}|\beta\rangle\langle\beta|\hat{D}|3d\rangle}{\omega_\beta - \omega} + \frac{\langle 3s|\hat{D}|\beta\rangle\langle\beta|\hat{D}|3d\rangle}{\omega_\beta + \omega} \right\} \qquad (4.1)$$

where Δ_s is the a.c. Stark shift, E is the electric field strength of the laser, ω is the frequency of the laser field, and $\hat{D}$ is the dipole

operator between the states in the bracket. The letter β represents any allowed one-photon transition from either the 3s or 3d states, ω_β is the resonance frequency between the 3s state and β, and $\hbar$ is Planck's constant.

The reduced one-photon Rabi frequency, which represents the rate of oscillation between states a and b, is defined as (Hurst and Payne, 1988).

$$\Omega_1(a\text{-}b) = E|D_{ab}|/2\hbar \tag{4.2}$$

where $|D_{ab}|$ is the dipole matrix element between the states a and b. Using this notation Eq. (4.1) becomes

$$\frac{\Delta_s}{2} = \sum_\beta \left\{ \frac{\Omega_1(3_s\text{-}\beta)\Omega_1(\beta\text{-}3d)}{\omega_\beta - \omega} + \frac{\Omega_1(3_s\text{-}\beta)\Omega_1(\beta\text{-}3d)}{\omega_\beta + \omega} \right\} . \tag{4.3}$$

Although this is an infinite sum over all β states, one term dominates because the laser frequency is relatively close (2400 cm^{-1}) to the 3s-3p resonance frequency. Therefore, for the purposes of this experiment, the a.c. Stark shift may be approximated as:

$$\frac{\Delta_s}{2} = \frac{\Omega_1(3s\text{-}3p)\Omega_1(3p\text{-}3d)}{\delta_\beta} \tag{4.4}$$

where δ_β is the detuning of the laser frequency from the 3s-3p resonance frequency. The laser energy measured was 0.3 mJ/pulse (pulse length = 4 ns) and had a beam radius of 0.15 cm. This was focused into the heat pipe by a 35 cm focal length lens. The intensity of the beam (which is proportional to E^2) is

2.88×10^7 W/cm^2. The matrix element $|D_{ij}|$ may be calculated from the oscillator strength between the states (see Hurst, 1988, for details of the calculation). The magnitude of the a.c. Stark shift due to the laser beam is 0.0154 cm^{-1} at this pump intensity.

This is much smaller than the laser bandwidth (0.04 cm^{-1}) which is evidence that the Stark shift due to the laser beam is insufficient to cause any dramatic effect. However, another source of radiation couples the 3d and 3p states, the ASE and SHR emissions which are resonant or nearly so. There is now a strong interaction between this radiation and the atoms. This results in a linear a.c. Stark effect (Bakos, 1977) which may be calculated from the one-photon reduced Rabi frequency between the 3p and 3d states (see Eq. (4.2)). This is also often referred to as the classical Autler-Townes effect (1955).

The SHR emission was measured in the laboratory to have an intensity of 1.23×10^4 W/cm^2 at a sodium vapor pressure of about one torr and a laser intensity of about 3×10^7 W/cm^2. Following the procedure outlined in Hurst and Payne (1988), the one-photon Rabi rate for the SHR-ASE radiation is 2.43×10^{10} rad/sec, or equivalently, 0.129 cm^{-1}. The linear Stark shift is twice this large. This is significantly greater than the bandwidth of the laser (0.04 cm^{-1}). Thus, ASE production will be dramatically reduced because the a.c. Stark effect has pushed the 3d resonance outside of the frequency range of the laser.

This leads to the question of exactly how one defines ASE under circumstances where resonances are moving around as a result

of a large Stark shift. If ASE involves resonance behavior, then the a.c. Stark shift can cause the laser to detune from the two-photon resonance by more than a laser bandwidth, which turns two-photon pumped ASE into SHR. The situation is confusing. The only thing that is clear is that there is an ambiguity in defining ASE and SHR when electric fields are present of sufficient intensity to cause a significant a.c. Stark shift. Significant in this context being defined as greater than the bandwidth of the laser.

The large a.c. Stark shift due to the SHR emission has led to an interesting modeling of the a.c. Stark-related behavior of the SHR emission. If one is detuned a great deal from resonance, the intensity for SHR production decreases according to $1/\delta^2$ (Hurst and Payne, 1988). A physical picture for this dependence is as follows. For SHR production, the laser is detuned from the upper resonance by δ. In addition, the generated SHR emission is also detuned δ from the resonance frequency between the upper and lower states. Therefore, the SHR production is limited by the quantity δ^2.

Assuming that the laser itself has a nonuniform intensity profile in time, the SHR emission will not fluctuate. At times of high laser intensity and high SHR production the Stark shift is large and cuts off production of the SHR process. At low SHR intensities the a.c. Stark shift is small and the intensity of the SHR process remains high. So while the laser intensity profile may fluctuate, the SHR intensity profile grows to be more nearly uniform as it propagates backward along the laser beam. Payne et al. (1988) have

put these types of intensity profiles into a model for SHR production that includes the a.c. Stark effect. The predictions include (1) the backward SHR signal should increase only linearly with laser intensity provided there is no significant absorption of the laser beam (i.e., at moderately low pressures, see Figure 3.3, p. 52), (2) there is a particular frequency profile for the backward SHR emission that changes as a function of sodium vapor pressure, and (3) the maximum backward SHR intensity for various pressures at a fixed laser intensity. All of these predictions agree well with the present data.

Payne et al. (1988) have predicted a reduction factor that controls the production efficiency of the backward SHR emission. Inherent in the approximations used is a nonzero finite laser bandwidth. The reduction factor has the form:

$$R = \frac{(2\Gamma_L)^2}{(2\Gamma_L)^2 + (\frac{\Omega_R}{\delta})^2} \tag{3.6}$$

where Γ_L is the bandwidth of the incident laser, Ω_R is the one-photon Rabi rate associated with the SHR emission (which is proportional to the a.c. Stark shift), and δ is the detuning of the laser from the two-photon resonance frequency.

The reduction factor becomes important when the Stark shift becomes larger than $2\Gamma_L$. On the basis of this study it is maintained that it is this reduction factor that limits the production of the

SHR in the backward direction shown in Figure 3.3 (p. 52) rather than the two-photon interference effect which was disproven in the laser absorption experiment described above. Both the line profiles and the maximum SHR output at different sodium pressures predicted by this model match those determined experimentally to rather surprising degree of accuracy. Consider SHR emission associated with near-resonant pumping of the 4d states. Scans of the backward 23,000 Å emission at both high and low sodium vapor pressure are shown in Figure 3.4. The dip near the resonance position corresponds to exactly what one would expect when including the a.c. Stark effect in the amplitude calculation for the backward SHR emission (see Figure 3.5). The asymmetry of the dip seen in the experimental results can be explained in terms of a FWM process that was ignored in the theoretical calculation (Payne et al., 1988).

The explanation for the dip is as follows. In addition to the backward SHR process there exists a FWM signal in the forward direction. As will be explained further in the next chapter, there is a phase-matching point for the FWM emission that is located slightly above the $3p_{3/2}$ resonance. When one is detuned to the high energy side of the resonance, there is a point close to the 4d resonance that coincidentally produces radiation that is almost exactly resonant with the 4d and 4p states even though neither of the virtual states associated with the PFWM signal are at the atomic resonance positions. This radiation causes a large Stark shift because it is nearly resonant. This suppresses the production of the

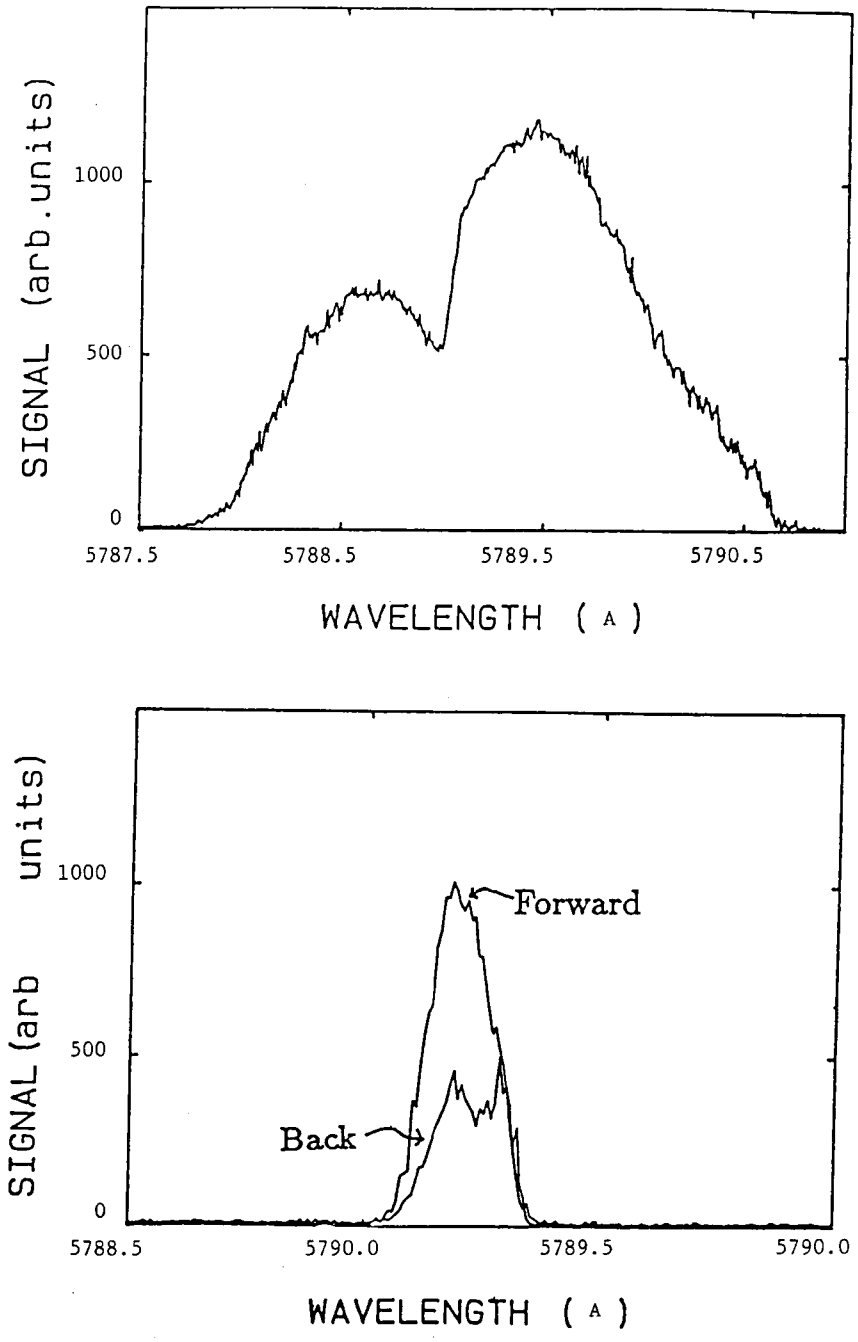

Figure 3.4. Backward hyper-Raman emission profiles as laser is tuned across two-photon 3d resonance. Sodium vapor pressure at (a) 1.5 torr and (b) 0.007 torr. E ≃ 3 mJ/pulse. SHR emission is at λ = 23,000 Å.

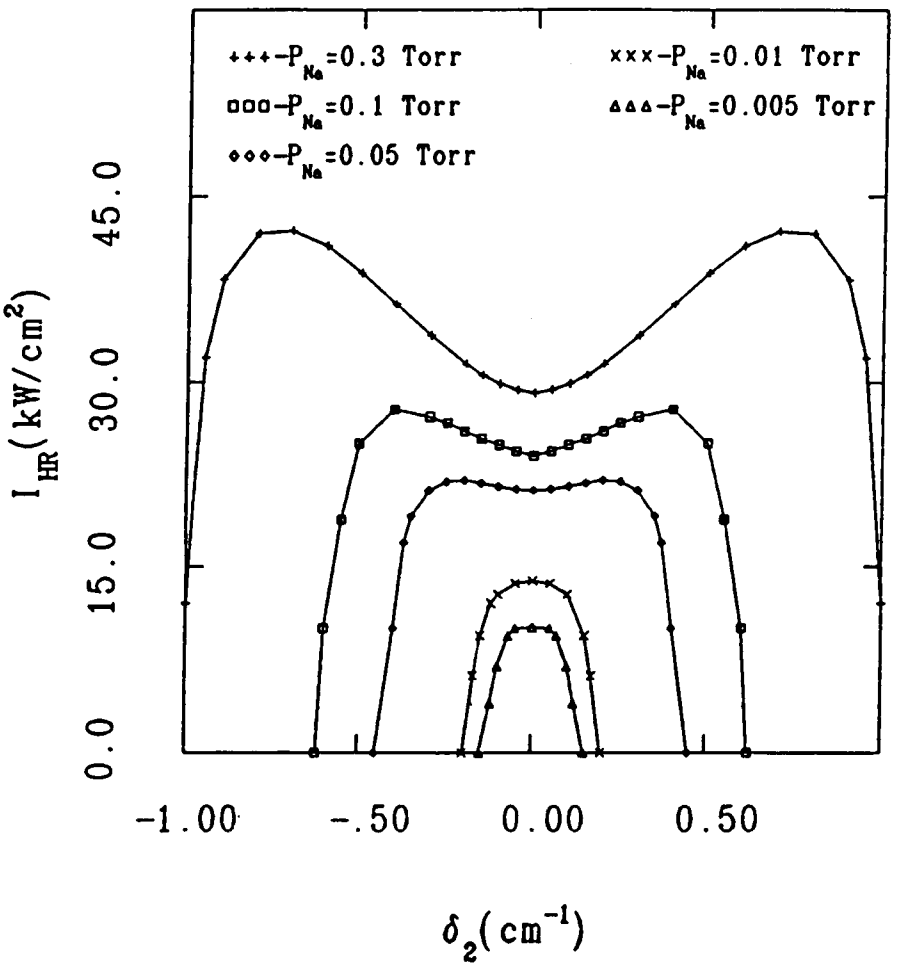

Figure 3.5. Theoretical predictions of SHR profiles that include the a.c. Stark effect. (Plot courtesy of M. G. Payne.) The intensity of the backward SHR emission from the 4d-4p transition is plotted as a function of detuning the laser from the two-photon 4d resonance. Each curve represents a different sodium vapor pressure.

backward SHR in this frequency region. The forward emission in Figure 3.4b is not produced by an SHR process since hyper-Raman emission is suppressed by the interference described in Chapter II, but rather it is an axially propagating FWM signal that will be explained in the next chapter.

C. Conclusions

The a.c. Stark effect plays an important role when dealing with the behavior of a nonlinear medium such as sodium in regions around narrow atomic resonances. In fact the role is so significant that to ignore it leads to erroneous theoretical predictions. In the observations of the suppression of ASE seen by Malcuitt et al. (1985), it is not necessary to invoke an interference effect between ASE and FWM to get the reduction in ASE intensity. At low-laser intensity when the Stark shift is not yet significant, the three-photon/one-photon interference effect described in Chapter II eliminates the forward SHR. It is only at fairly high-laser intensities that Malcuitt et al. (1985) saw the ASE suppression effect. At high SHR intensities there is sufficient energy to create a Stark shift large enough to suppress the process. Furthermore, the a.c. Stark effect is evident in every case where there is nearly resonant light coupling two states. Therefore, this suppression should be equally evident in the case of the two-photon 4d resonance with SHR emission to the 4p state. Malcuitt et al. did not observe this to be the case. However, this can be explained by another phenomenon discovered while doing

work on the suppression effect described in Chapter II. The process is axially phase-matched PFWM and it will be the topic in the next chapter.

CHAPTER IV

GENERATION OF AXIALLY PHASE-MATCHED PARAMETRIC FOUR-WAVE MIXING

A. Theoretical Considerations

In Chapter II a pertinent question was how to distinguish between two nonlinear optical phenomena which occur simultaneously from multiphoton excitation of moderately dense alkali vapors. Specifically, it was necessary to separate the SHR process from the accompanying parametric four-wave mixing (PFWM) signal in the forward direction. As was discussed in Chapter I, emission from the SHR process, which leaves an atom in an excited state, propagates along the axis of the laser beam in either the forward or backward direction. In contrast, PFWM processes (see Figure 4.1) will only produce constructively interfering wavefronts if the photons propagate at an angle to the incident beam axis. This situation exists because PFWM emission and the laser radiation have different frequencies and, therefore, different indices of refraction in the medium. Propagation at a cone angle allows phase-matching or constructively interfering wavefronts to occur.

Distinguishing between SHR and PFWM processes may be accomplished in either of two ways. One can take advantage of geometric aspects of the two types of propagation to separately detect the two types of emission. Specifically, one can eliminate

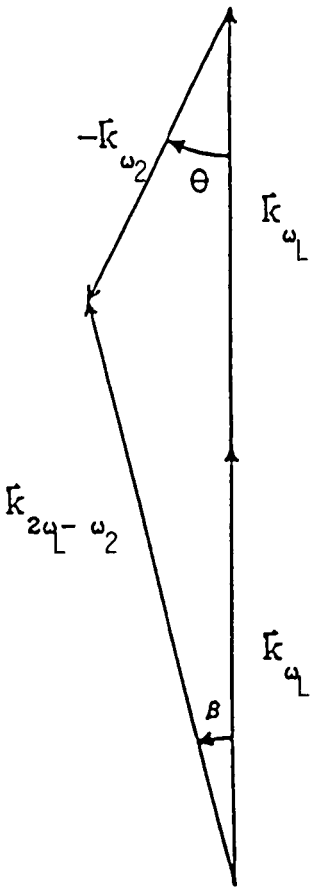

Figure 4.1. Conical angle-matched parametric four-wave mixing. Two laser photons of frequency ω_L induce the medium to produce phase-matched radiation at frequencies ω_2 and $2\omega_L-\omega_2$ that propagate conically out of the medium.

the conically emitted PFWM light by putting a small aperture in the forward beam. Detectors then see only emissions produced at near zero angle of propagation. Conversely, one may put a small beam block of approximately the same size as the aperture in the center of the laser beam, thereby excluding the axial component at zero angle of propagation from a downstream detector. The remaining conical FWM emission may be collected by a lens and focused into a suitable photon detector.

Alternatively, one may distinguish between the SHR and PFWM processes by wavelength discrimination. Since the FWM signals are produced at frequencies slightly different from those associated with atomic excitation by SHR emission, the two processes may be distinguished by their respective wavelengths with a spectrometer of sufficient resolution. Note in Figure 1.4 (p. 18) that PFWM must occur at a small detuning, δ, from the odd parity state, whereas the SHR process occurs exactly on that resonance.

Under certain combinations of laser energy density and atomic vapor pressure in the present studies an anomaly arose when the wavelength profile of the axial part of the forward beam was examined. In a spectral scan of emissions occurring at a fixed laser pumping frequency, an extra, and rather confusing, peak appeared at a wavelength between the expected SHR peaks when the laser was tuned close to two-photon resonance with the 3d or 4d states. Moreover, the photons associated with the extra peak propagated axially, typical of the SHR process, not conically as in PFWM. This extra peak was

not always there. In the 3d case it occurred only when operating at sodium vapor pressures above 1.5 Torr, or at lower pressures when the laser beam was focused into the heat pipe.

In the 4d case a similar "extra" peak appeared at pressures as low as one torr without the laser beam being focused. However, laser energy densities available in the 4d case were much higher than those for the 3d because a more efficient dye was available in this frequency region.

What are the conditions necessary for phase-matched axial propagation of all four waves in PFWM (see Figure 4.2)? As was discussed in Chapter I, the phase relation between the various waves, as governed by their propagation through the nonlinear medium, is determined by the magnitude of the propagation vectors of the separate waves,

$$|\vec{k}_\alpha| = \frac{2\pi}{\lambda_\alpha} = 2\pi\nu_\alpha n = \frac{\omega_\alpha n}{c} = \frac{\omega_\alpha}{v} \qquad (4.1)$$

where ν_α is the frequency of the light, λ_α is its wavelength, n_α is its index of refraction in the medium, and c is the speed of light in a vacuum. Alternatively, $\omega_\alpha = 2\pi\nu_\alpha$ is the "angular frequency" of a given wave and v is its phase velocity. For phase-matched parametric four-wave difference mixing to occur, the k vectors of the four waves must satisfy the relation $2\vec{k}(\omega_L) - \vec{k}(\omega_2) = \vec{k}(2\omega_L - \omega_2)$. This guarantees constructive interference of the waves, but does not mean that all four waves will propagate axially along the laser axis.

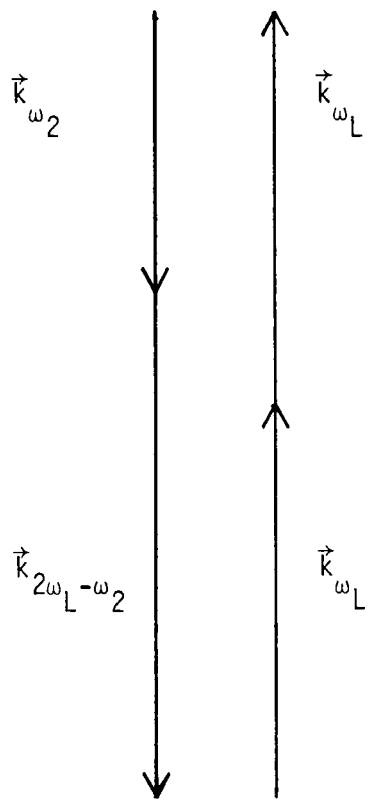

Figure 4.2. Axially phase-matched parametric four-wave mixing. Under certain conditions, propagation of the generated photons (at ω_2 and $2\omega_L-\omega_2$) are axial due to the dispersive properties of the medium.

In fact, waves generated in PFWM processes generally adjust their angle of propagation (as described in Chapter I) to satisfy this relation.

For axial propagation (all waves parallel or antiparallel) another constraint must be put on the k vectors. It is necessary that the magnitudes of the k vectors obey the following relationship:

$$|\vec{k}(2\omega_L-\omega_2)| = 2|\vec{k}(\omega_L)| - |\vec{k}(\omega_2)| \ . \tag{4.2}$$

Substituting from Eq. (4.1), and multiplying through by c gives:

$$(2\omega_L-\omega_2)n(2\omega_L-\omega_2) = 2\omega_L n(\omega_L) - \omega_2 n(\omega_2) \ , \tag{4.3}$$

which may be written as:

$$(2\omega_L-\omega_2)[n(2\omega_L-\omega_2) - 1] + 2\omega_L-\omega_2$$
$$= 2\omega_L[n(\omega_L) - 1] + 2\omega_L-\omega_2[n(\omega_2) - 1] - \omega_2 \ . \tag{4.4}$$

Using

$$4\pi N\alpha = n^2 - 1 = (n-1)(n+1) \ . \tag{4.5}$$

In a gas vapor n remains near one so that $n + 1 \simeq 2$ except within a few atomic widths of the resonance. Now Eq. (4.5) becomes

$$[n(\omega) - 1] = 2\pi N\ \alpha(\omega) \tag{4.6}$$

where $\alpha(\omega)$ is the mean microscopic polarizability and N is the number density of the medium (Born and Wolf, 1975). Then Eq. (4.4) becomes

$$(2\omega_L-\omega_2)\alpha(2\omega_L-\omega_2) = 2\omega_L\alpha(\omega_L) - \omega_2\alpha(\omega_2) \tag{4.7}$$

When conditions in Eq. (4.7) are met, PFWM light can be generated at ω_2 and at $2\omega_L-\omega_2$ by two laser photons at ω_L, and the generated waves will travel in phase down the axis parallel to the laser beam because the difference in the k vectors, Δk, is zero and the magnitude of the k vectors satisfy Eq. (4.2).

In general, the index of refraction, n, of a medium increases with frequency. This is called normal dispersion. The index may be calculated for any medium at any frequency if enough of the oscillator strengths coupling populated states to upper states are known. Then

$$n^2(\nu) - 1 = \sum_i \frac{F_i}{\nu_i^2-\nu^2} \tag{4.8}$$

where n is the index of refraction at the frequency ν, F_i is the oscillator strength of any one-photon allowed transition with a populated state, and ν_i is the resonance frequency of the allowed transition (Born and Wolf, 1975). Using the approximation that $n^2 - 1 \simeq 2(n-1)$ in vapors, and rewriting Eq. (4.8) in terms of wavelengths instead of frequencies:

$$n(\lambda) - 1 = K \sum_i \frac{F_i}{\frac{1}{\lambda_i^2} - \frac{1}{\lambda^2}} \tag{4.9}$$

where K is a constant for dimensional consistency.

For sodium the oscillator strengths and transition wavelengths are known and the index for any frequency may be easily calculated with rather good accuracy using a simple computer program. Frequencies near resonances exhibit "anomalous" dispersion due to the strong absorption of these frequencies by the medium. Here the index goes through a sharp drop and the quantity $\alpha = (n-1)/2\pi N$ goes through a sign change (see Figure 4.3).

As a case in point, consider Figure 4.3. When pumping to the two-photon 4d resonance, the frequency of the laser photons is on the high energy side of the 3p resonances. This is in a negatively dispersive region (i.e., the quantity α is negative). The light generated at ω_2 is in the infrared range ($\lambda \simeq 8200$ Å), far from any resonance frequency. Although $\alpha(\omega_2)$ is slightly positive, it is very close to zero and in a region where α does not change appreciably over a long wavelength region. For light to be generated both at $2\omega_L - \omega_2$ and ω_2, and propagate in phase with the driving frequency, ω_L, it is necessary for them both to adjust their wavelengths so that the microscopic polarizations, α, and the frequencies satisfy Eq. (4.7).

In the region of the p resonances there are three places where α changes sign. Two of these regions are very narrow and correspond to exact resonances (labeled a and c on Figure 4.3). The laser frequency, ω_L, may be in either a negatively or positively dispersive region. When pumping the two-photon 4d resonance it is in a negatively dispersive region; in the two-photon 3d resonance case it is in a positively dispersive region. Constructively interfering

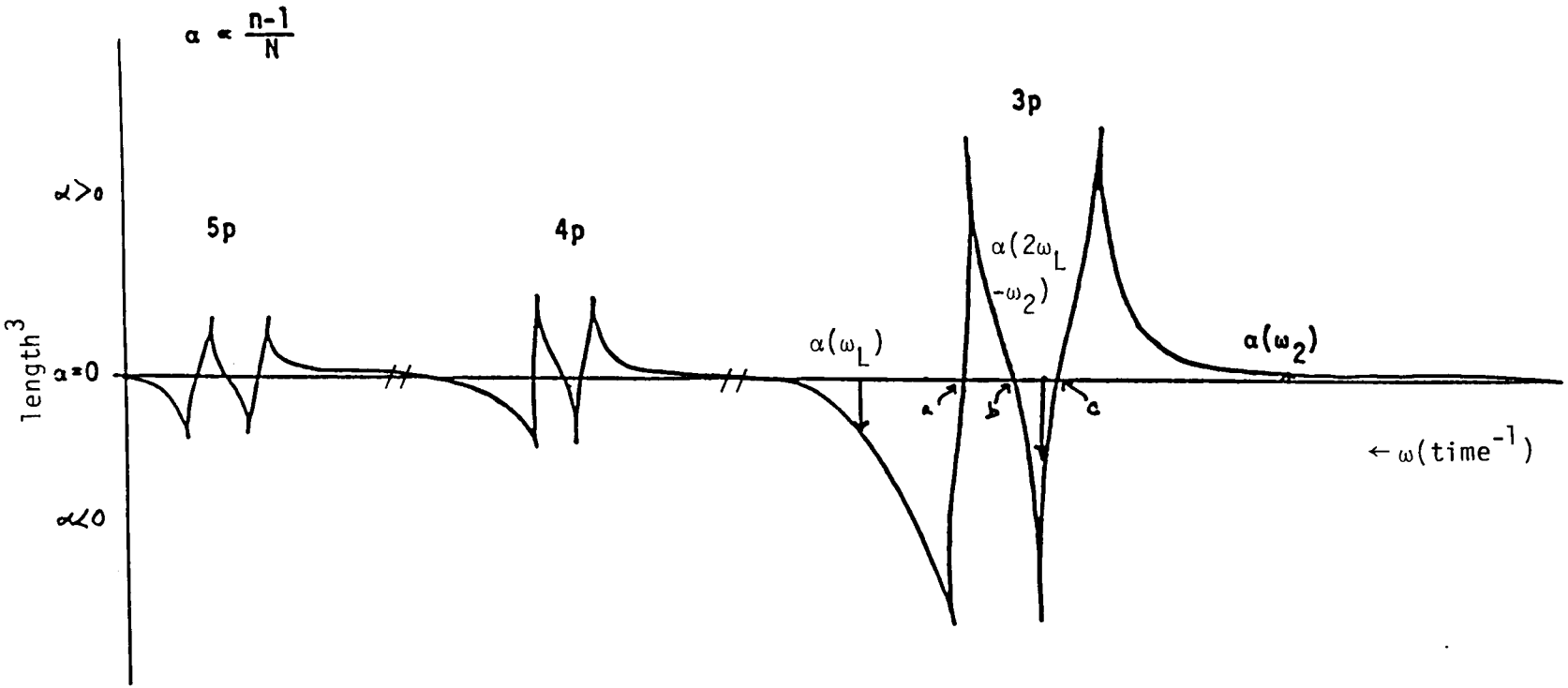

Figure 4.3. Regions of anomalous dispersion across one-photon resonances in sodium vapor. The figure is not to scale since the fine structure levels within a state are very close together. In addition, the amplitude of the dispersion for the 3p states is 80 times that for the 4p state due to the differences in the oscillator strengths with the ground state. α is the microscopic polarization of the sodium vapor and ω is the frequency of the coupling radiation.

wavefronts can only occur when the indices of the laser photons and the produced emission allow phase matching to occur. This can happen in the narrow resonance frequency bands since the index takes on a very wide range of values over this very narrow frequency region. This is not, however, PFWM emission because it produces an exact resonant frequency. Instead it is ASE or SHR emission. In the region between the two resonance frequencies there is another place that α changes sign (labeled b). This is no longer a resonance frequency, and the PFWM process will find a frequency location where the indices allow the conditions in Eq. (4.7) to be satisfied.

Some controversy as to where the phase-matching point occurs has been seen (Krasinski, 1985). If the medium at the laser frequency had an index of exactly one, so that $\alpha(\omega_L)$ was equal to zero, the phase-matching point for the generated PFWM light would occur exactly at the zero crossing point. However, $\chi^{(3)}(\omega)$ is nearly zero at this point because the dominant contributions are from the nearby 3p fine structure levels which are nearly equal and of opposite sign (Shen, 1984). So even though the phase-matching condition is satisfied, there is no source term for this frequency and no emission will be produced at this frequency. Since the laser photons can never have an index of exactly one in the medium, this is not experimentally a problem. The experiments in the next section demonstrate the existence of the phase-matched axially propagating PFWM process.

B. The Experiments

Three of the four experiments to be described were performed in conjunction with work discussed in Chapter III involving the axial

propagation of SHR emission generated in two-photon excitation to virtual states near the 3d or 4d states. The experimental setup is shown in Figure 3.2 (p. 49) except that only the forward emission was examined.

In Figure 4.4b, the emission from the 4d-3p transition region is shown. The laser is detuned by 0.1 Å to the high energy side of the 4d two-photon resonance and left unfocused. Here the emitted light is collected by a quartz lens and focused into a spectrometer. Thus, one sees a wavelength profile of the entire beam, including both axial and conical emissions. Note the two outer peaks at λ = 5684.2 Å and 5689.7 Å which are near the $4d\text{-}3p_{1/2}$ and $4d\text{-}3p_{3/2}$ transition wavelengths, respectively. Notice the conspicuous additional peak in between the expected lines at an intermediate wavelength λ = 5686.1 Å. In Figure 4.4a a small (0.3 cm) aperture has been put in the forward beam with all other conditions remaining constant. The two outer peaks disappear while the center peak remains unchanged. Since the photons in the outer peaks no longer enter the spectrometer when the aperture is in place, they are conical FWM signals that result from PFWM which is generated through angle phase matching, and not SHR emission which travels down the axis of the laser as described in Chapter II. A forward SHR emission is not expected because of the suppression effect described in Chapter II. This middle peak is attributed to the axially phase-matched FWM process described in the previous section.

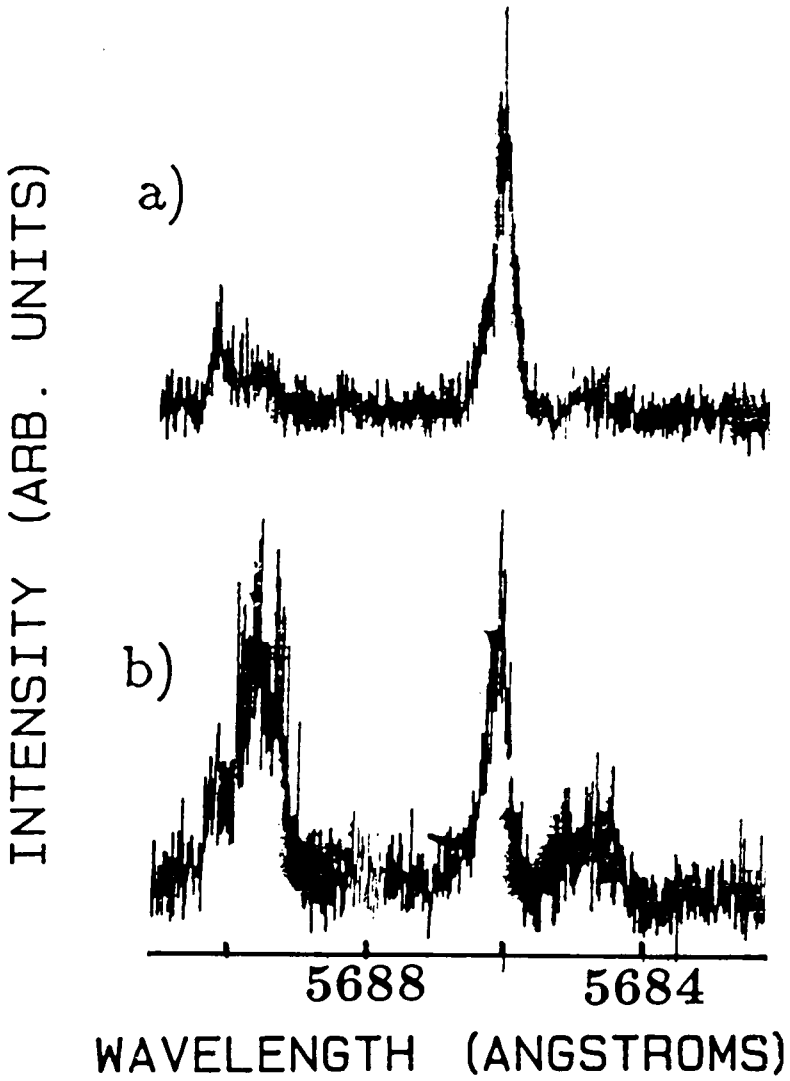

Figure 4.4. Emission from sodium 4d-3p transitions. (a) Axial component only, large peak at 5686.1 Å is an axially propagating PFWM signal, (b) axial and conical components combined, outer peaks are conically phase-matched PFWM signals from the $4d\text{-}3p_{3/2}$ (5688 Å) and $4d\text{-}3p_{1/2}$ (5683 Å), respectively. P = 1.5 torr, E = 5 mJ/pulse, δ = +0.1 Å.

As a test of the appropriateness of the FWM model, one can ascertain whether the four colinear vectors satisfying $\Delta k = 0$ at $\lambda = 5686.1$ Å satisfy the conditions set forth by Eq. (4.7). In this case:

$$\omega_2 = 17587 \text{ cm}^{-1} = 5686.1 \text{ Å} \qquad \alpha(\omega_2) = -2.7 \times 10^{-21} \text{ cm}^3$$
$$\omega_L = 17274 \text{ cm}^{-1} = 5788.8 \text{ Å} \qquad \alpha(\omega_L) = -4.2 \times 10^{-21} \text{ cm}^3$$
$$2\omega_L - \omega_2 = 16962 \text{ cm}^{-1} = 5895.6 \text{ Å}$$

A computer program was written to calculate the dispersion of sodium in any frequency region. It was assumed that the entire population of atoms remained in the 3s ground state, so that only one-photon allowed transitions from this state had to be included in the sum term of Eq. (4.9). The accuracy of α is limited by the accuracy of the oscillator strengths which averages approximately 20%. The dispersion for frequencies ω_L and ω_2 were determined and are listed above. The right hand side of Eq. (4.7), which sets the conditions for axially phase-matched PFWM, has a numerical value of -1.1×10^{-16} cm^2. The quantity is equal to $(2\omega_L - \omega_2)\alpha(2\omega_L - \omega_2)$ The wavelength of the complementary beam at frequency $(2\omega_L - \omega_2)$ is fixed at 5895.6 Å due to energy conservation principles. Therefore, $\alpha(2\omega_L - \omega_2)$ must be equal to $-1.1 \times 10^{-16}/(2\omega_L - \omega_2) = -6.6 \times 10^{-21}$ cm^3 if Eq. (4.7) is to be satisfied. If one uses the computer program to calculate the dispersion curve in this frequency region $(2\omega_L - \omega_2)$, α equals -6.6×10^{-21} cm^3 at 5894.7 Å. Within the resolution of the spectrometer, this wavelength and the $(2\omega_L - \omega_2)$ wavelength calculated

at 5895.6 Å are indistinguishable. This is a nonresonant wavelength and should, therefore, be visible in spectrometric scans of this wavelength region.

The wavelengths assigned for ω_2 and ω_L assume that the laser frequency, ω_L, remains at its vacuum wavelength while in the sodium vapor zone. In fact, this is not the case. At the laser frequency the quantity $\alpha(\omega_L)$ is negative which means that $\vec{k}_L$ is slightly shorter than it would be under vacuum conditions. Therefore, $2\omega_L-\omega_2$ would have a slightly shorter k vector, or equivalently a slightly longer wavelength while in the vapor zone. If one looks at the scans of the axial beam in the region of $2\omega_L-\omega_2$ (Figure 4.5), one notices a small "lump" in a region around 5894.5 Å which may very well represent the fourth wave in the axial FWM process that contains ω_2 = 5686.1 Å. Although this lump is small it must be remembered that many routes access the ground state through the 3p states, and it is not possible to isolate the part resulting only from the process described above.

Figure 4.6a shows the axial emission from the 3d-3p levels when tuned exactly to the 3d two-photon resonance in an unfocused geometry. The outer peaks at $\lambda \simeq$ 8185 Å and 8197 Å have an ASE component to the $3p_{1/2}$ and $3p_{3/2}$ states, respectively. Again, the small peak in between at 8188.6 Å is the phase-matched axial PFWM signal. Following the procedure described above in the 4d case, within the resolution of the spectrometer, Eq. (4.7) is again satisfied.

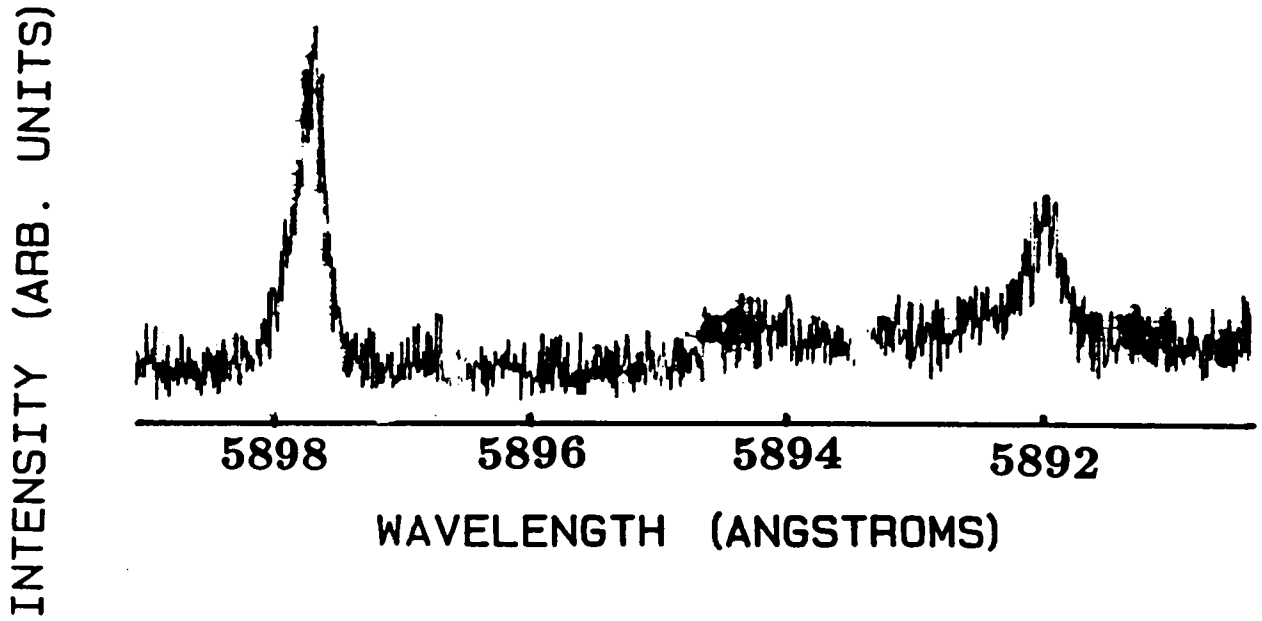

Figure 4.5. Axial and conical emissions from sodium in the region of 3p-3s transitions when tuned to the two-photon 4d resonance. P = 0.4 torr, E = 5 mJ/pulse. Peaks at 5897.5 Å and 5892 Å are combined ASE, SHR, and conical PFWM emission from $3p_{1/2}$ and $3p_{3/2}$ levels, respectively. The small "lump" at 5894 Å is axial PFWM emission.

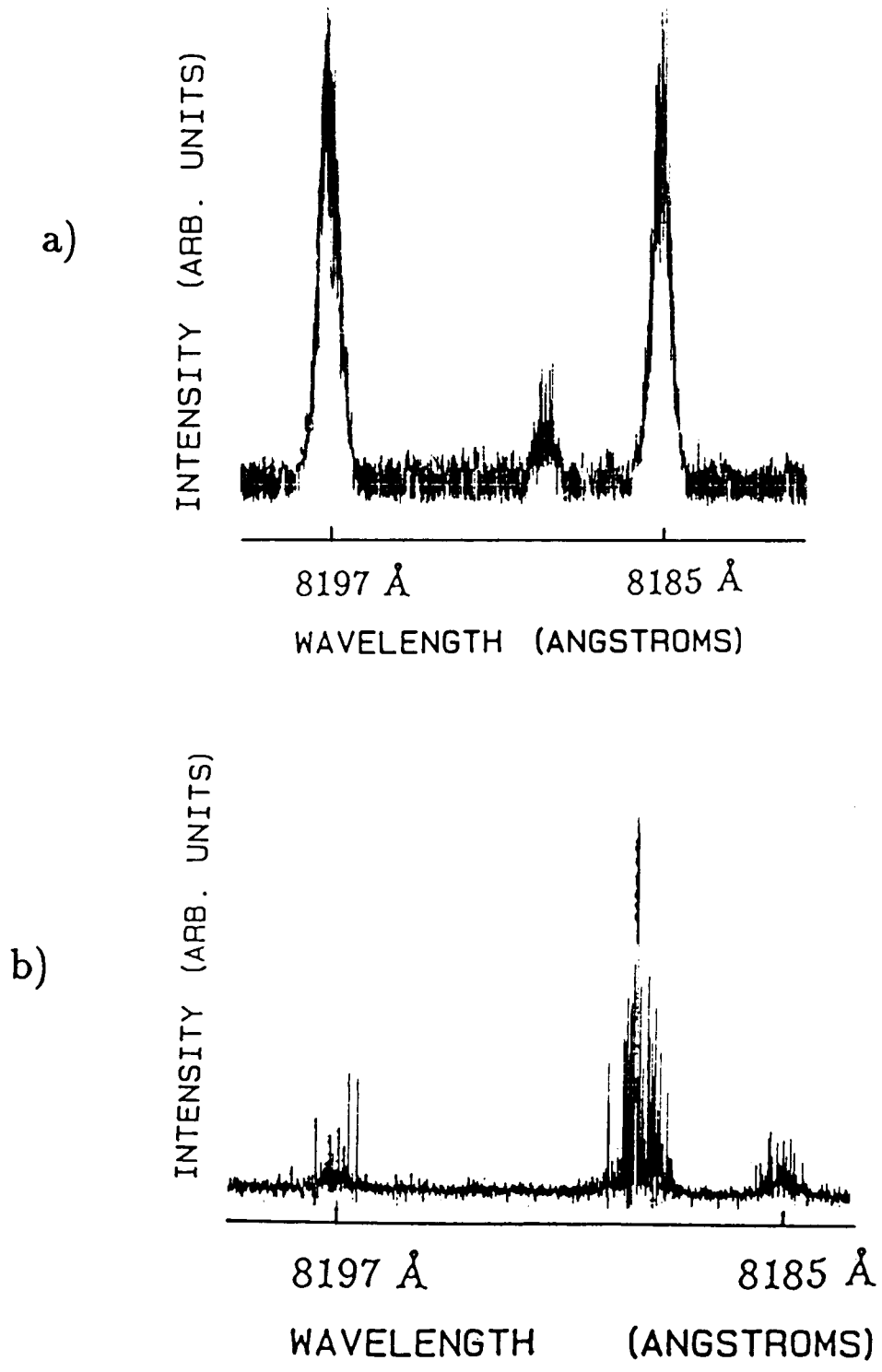

Figure 4.6. Axial emission of sodium in region of 3d-3p transition in an unfocused geometry when tuned to the two-photon 3d resonance. Sodium pressure (a) 2 torr, (b) 3 torr. The outer peaks in both figures are combined ASE and SHR emission from the 3d-$3p_{3/2}$ and 3d-$3p_{1/2}$ states, respectively. The center peak at 8188.6 Å is an axial PFWM signal.

Figure 4.6b shows another case of axially propagating PFWM out of the 3d state using an unfocused geometry, this time under conditions of higher sodium vapor pressure. Notice that the axial four-wave mixing signal is actually larger than the ASE/SHR emission peaks found to either side. As explained in Chapter III, the ASE is suppressed by the a.c. Stark effect. The PFWM signal is less affected by the shifting of resonances since it is already a nonresonant process. To confirm that this emission was actually PFWM, a search was made for the complementary wave at $2\omega_L-\omega_2$. In the region of 5895.5 Å (yellow) a complementary axial emission was found. Both axial emissions at ω_2 and $2\omega_L-\omega_2$ disappeared when the pressure was lowered to approximately 1.5 torr.

Figure 4.7 shows emissions associated with the 3d-3p levels at various laser detunings under a focused geometry. In Figure 4.7a the laser is tuned exactly to the two-photon 3d resonance and focused into the center of the heat pipe by a 35 cm focal length lens. The axial FWM peak at λ = 8189.3 Å is quite large. When the laser is detuned 0.4 Å (Figure 4.7b) to the high energy side of the two-photon resonance, the axial FWM piece is even larger than the emissions on either side of it. It is also closer to the right hand side peak than it was at zero detuning. However, when detuned by 0.7 Å as in Figure 4.7c, the axial FWM piece has disappeared while there remains a weak signal near the expected resonance positions.

Since the laser beam is focused, it is not clear to which process the outer peaks should be attributed. The two outer peaks

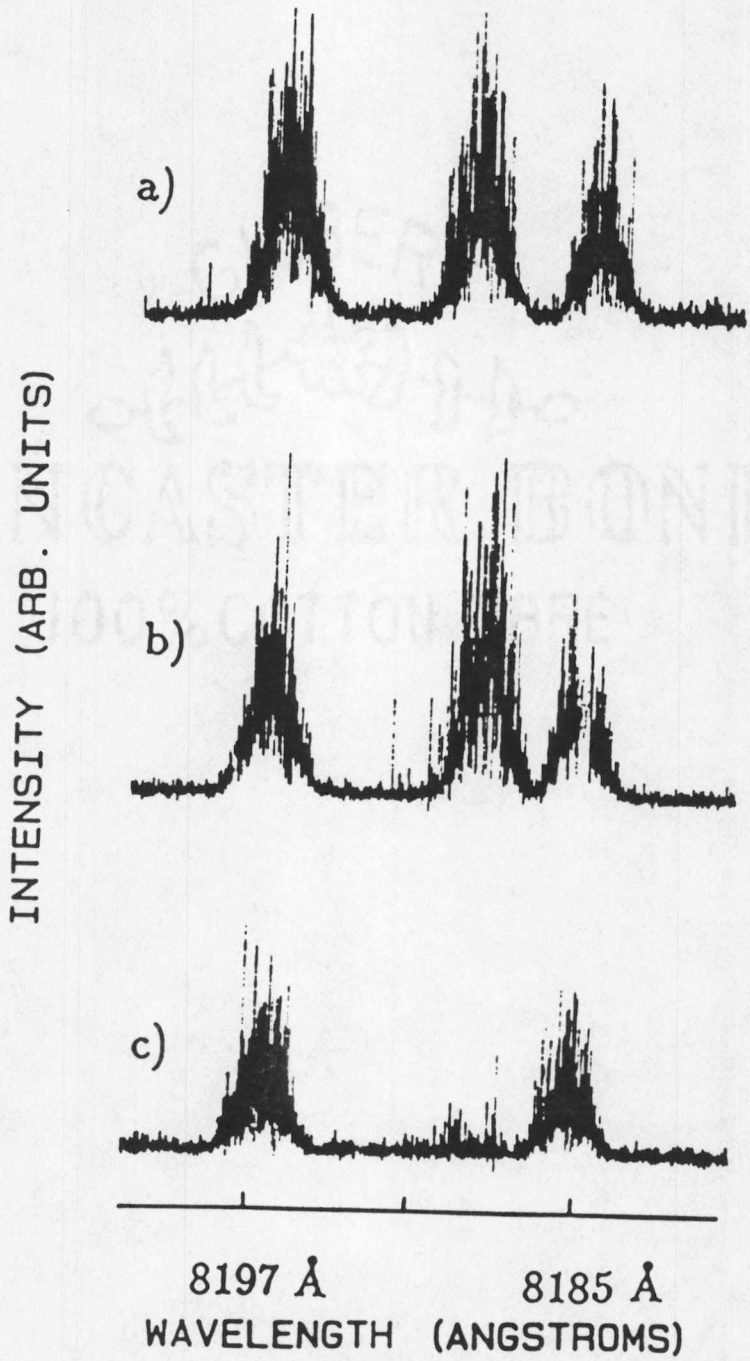

Figure 4.7. Axial emission in region of 3d-3p transition in sodium under a focused geometry at various laser detunings from two-photon 3d resonance. (a) 0 Å, (b) 0.4 Å, (c) 0.7 Å. P = 1.5 torr, E = 0.6 mJ/pulse. Outer peaks are due to ASE and SHR emission to $3p_{3/2}$ and $3p_{1/2}$, respectively, with some component of angle-matched PFWM. Center peak is axial PFWM. The shift in relative peak spacing is due to population transfer changing the index of refraction of the medium and thereby changing the conditions for phase matching.

have a wider spectral profile than the corresponding ASE peaks in the unfocused geometry. This fact along with the shifting of the relative spacing between the center and outer peaks leads to the conclusion that one does not see a pure SHR or ASE process for the outer peaks. Instead, it is a mixture of the conical PFWM signals, SHR emission, and ASE. Since the laser beam is focused, the concept of well-defined cone angles for FWM processes becomes less meaningful. Krasinski et al. (1985) have briefly reported this phenomenon in a paper dealing with other aspects of this system under similar experimental conditions. However, they did not realize the mechanism for the production of the axial portion of their signal which this study has shown to be axially phase-matched PFWM. Applying Eq. (4.7) to test the axially propagating four-wave mixing model becomes impractical since the wavelength of the axial PFWM peak cannot be accurately ascertained. In addition, there is evidence that under the conditions imposed by a focused geometry, population transfer to the 3p states has occurred. This evidence consists of spectral scans of backward 3p-3s emission. If no population transfer occurs, emission of this frequency (exactly resonant ASE) would be totally absorbed by the medium. The amount of transfer radically alters the index of the medium, and the simple model where all atoms remain in the ground state becomes inadequate. This evidence is presented in the second section of Chapter V.

Axially phase-matched PFWM in an unfocused geometry can be demonstrated further by examining another path from near the 4d

two-photon resonance to the ground state. This path goes by way of the 4p states and avoids the 3p states completely. Here ω_2 is light generated from the near 4d to the near $4p_{3/2}$ or $4p_{1/2}$ levels and is in the infrared range with λ = 23,300 Å. The wave at frequency $2\omega_L-\omega_2$ is in the UV range where $4p_{3/2}$-3s and $4p_{3/2}$-3s transitions have λ = 3302.3 Å and 3302.9 Å, respectively. Since the spectrometer used for the UV data has at best a resolution of 0.3 Å, it is difficult to spectrally resolve components of axial FWM and regular angle-matched FWM processes. The spectral resolution possible for the 23,300 Å light was substantially worse. However, qualitative differences can be seen in Figure 4.8 for the UV process. Figure 4.8a shows the whole UV beam, both axial and conical emissions. Figure 4.8b shows only the axial part, while Figure 4.8c shows only the conical emission, where these results were obtained through the use of pinhole and disk beam stops, respectively, as described earlier. Comparing Figure 4.8b and Figure 4.8c to Figure 4.8a, it is evident that there are at least four signals involved in the spectral scan in Figure 4.8a, two axial peaks and at least two conical peaks. Because of phase-matching considerations the axial and conical components cannot have the same wavelengths. However, they can be close together because the oscillator strengths of the 4p-3s transitions are very weak. Since there is no indication of a backward UV beam, the forward beam can only have FWM processes associated with it. Since one sees a definite pair of peaks associated with the axial parts of the signal, these must be axial

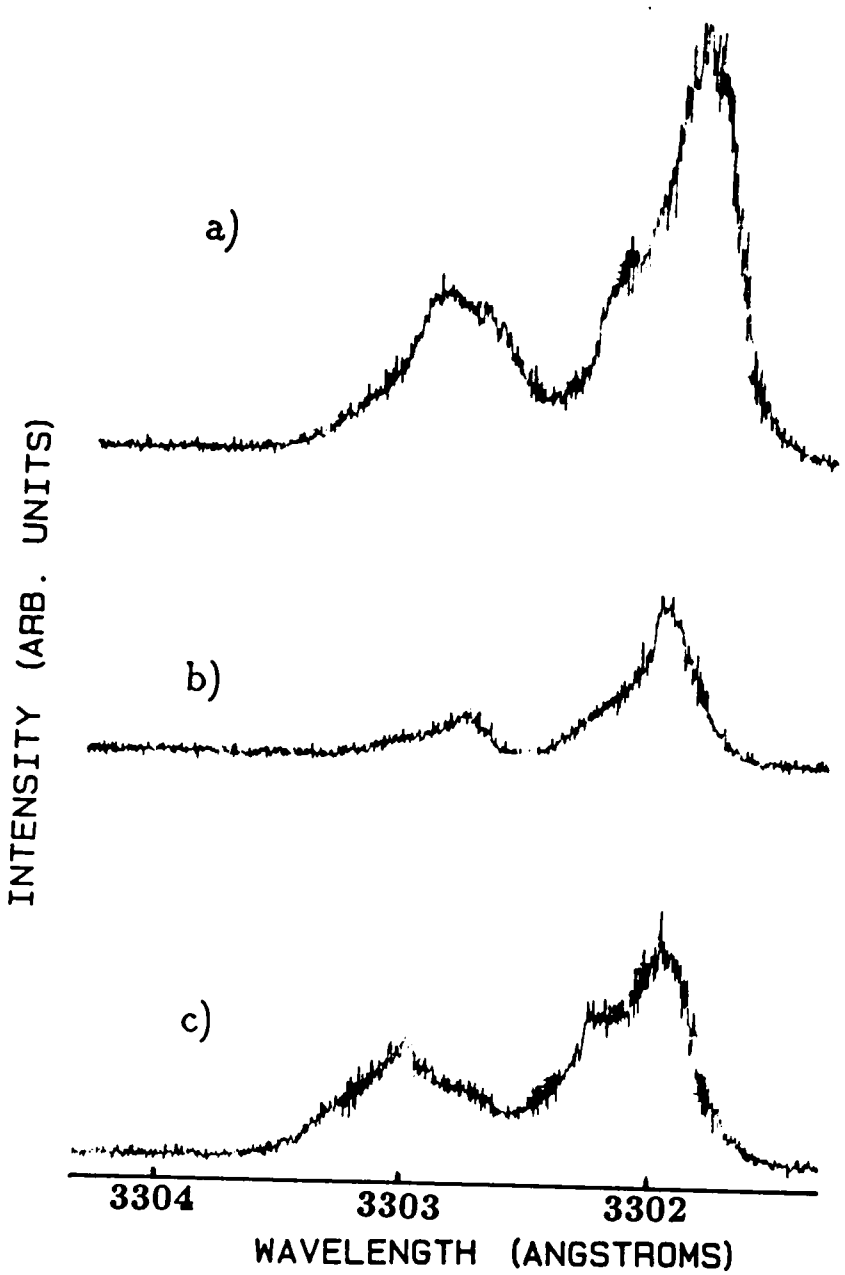

Figure 4.8. Ultraviolet PFWM signals from sodium 4p-3s transition. (a) Total forward emission, (b) axial emission only, both peaks due to axial PFWM, (c) conical emission only, four peaks due to conical PFWM. P = 0.8 torr, E = 1 mJ/pulse, δ = +0.4 Å.

FWM emissions rather than ASE or SHR signals, while the conical emission at slightly different wavelengths represent the angle-matched FWM signal.

But why are there two axial peaks instead of the one observed in the previous two cases? This can be explained if one examines the oscillator strengths of the 4p-3s transitions; they are very weak compared to the 3p-3s transitions (see Table 1.1, p. 10). If one calculates the dispersion in the region about the emission there are two positions where $\alpha(\omega_L) = \alpha(2\omega_L - \omega_2)$ which are very close to the resonant frequencies. One is between the resonances, the other is to the high energy side of the $4p_{3/2}$ state. In the other cases examined, the oscillator strengths connecting the upper states to the ground state were very strong. This pushes the other phase-matching position (the one not between the resonances) away from the region of the lower resonances and towards the next higher resonance state. However, if phase matching occurs far from the p states, any FWM generation will be very weak since the nonlinear susceptibility $\chi^{(3)}(\omega_2)$, becomes very weak far from the resonances (Shen, 1984). As was discussed in Chapter I, the source term for this other frequency, the polarization $P(\omega)$, is proportional to $\chi^{(3)}(\omega)$, $P(\omega)$ will also be vanishingly small and no detectable signal will be produced at this other phase-matching frequency. Thus one expects to see two axially propagating FWM signals near the 4p states, but only one near the 3p states. The four peaks associated with the 4p-3s transition have

been reported in the literature by Hartig (1978), but again like Krasinski, he did not recognize the mechanism for their production.

C. Conclusions

This study has led to the discovery of a new mechanism whereby phase-matched axial FWM processes may occur. These are FWM processes that do not use the angle adjustment to achieve phase matching, but rather take advantage of the dispersive qualities of the medium near resonances to match indices. This type of index matching results in propagation of PFWM emission down the axis of the laser beam in the forward direction. These emissions have been noted in the literature, but this is the first time they have been explained satisfactorily.

CHAPTER V

ADDITIONAL FINDINGS

A. Influence of A.C. Stark Effect on Backward Stimulated Hyper-Raman Profiles as a Function of Direction of Detuning from the Two-Photon 3d Resonance in Sodium Vapor

In Chapter II the suppression of forward stimulated hyper-Raman (SHR) emission due to parametric four-wave difference mixing was demonstrated. In doing the experiments necessary to demonstrate the suppression effect the laser was detuned from the two-photon 3d resonance, to both the high energy and low energy sides, and the forward to backward SHR emissions were compared. While analyzing the spectra taken it was noticed that the backward emission, which because of phase-matching considerations is composed of ASE and SHR, or SHR alone, had a peculiar asymmetric suppression of peaks depending on the direction of the detuning.

The emissions studied had wavelengths corresponding to transitions from on or near the $3d_{5/2,3/2}$ resonances to the $3p_{1/2}$ or $3p_{3/2}$ state at $\lambda \simeq 8185$ Å and 8197 Å, respectively. When the laser was tuned to the low energy side of the 3d states it was noted that the intensity of the 3d-$3p_{1/2}$ emission was always more suppressed than the 3d-$3p_{3/2}$ intensities (Figure 5.1b). The opposite would occur when detuned to the high energy side of the two-photon 3d

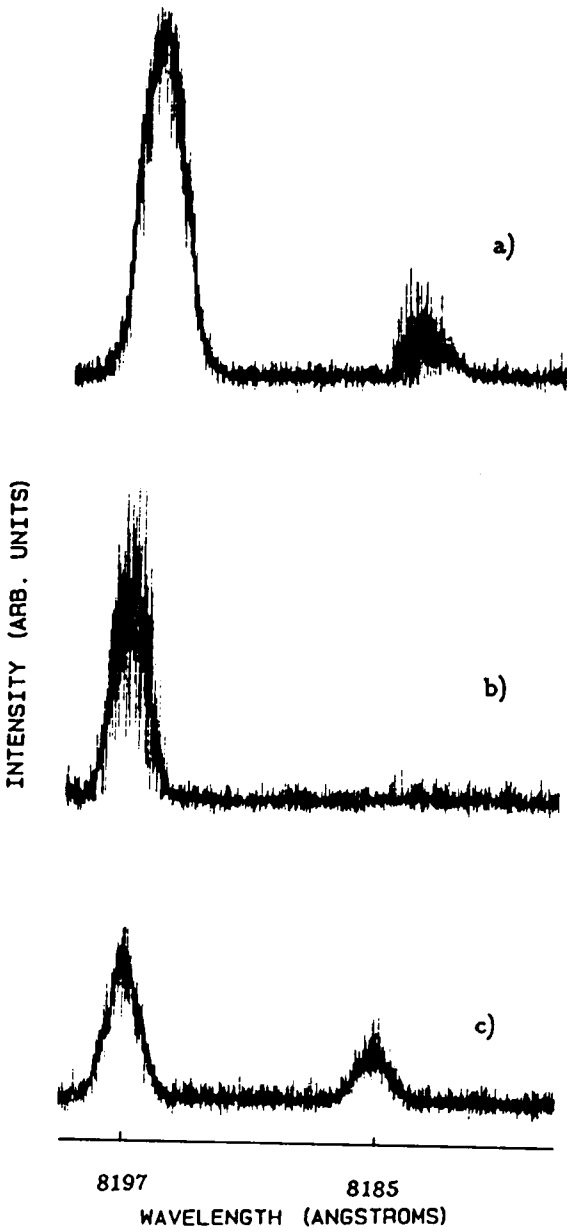

Figure 5.1. Backward SHR emission from 3d states to $3p_{3/2}$ and $3p_{1/2}$ states, respectively, at different laser detunings. (a) On resonance, (b) 0.3 Å to the low energy side, $3p_{1/2}$ transition suppressed, (c) 0.5 Å to the high energy side, $3p_{3/2}$ transition suppressed.

resonance; the $3d\text{-}3p_{3/2}$ peak was reduced in intensity more than the peak at 8185 Å (see Figure 5.1c).

The asymmetry of peak suppression due to the direction of incident laser detuning was puzzling, and consistently reproducible. It was some time before the reason for the asymmetry became evident. The reason became more obvious in light of the work done in Chapter III where the a.c. Stark effect was shown to cause the suppression of ASE.

The a.c. Stark effect causes either the apparent splitting or shifting of atomic levels because of the interaction between an electromagnetic field and an atom. The linear a.c. Stark effect is proportional to the product of electromagnetic field intensity and the dipole matrix element connecting two states, and occurs when resonant radiation couples two states. When the frequency of the radiation is far off resonance the effect becomes quadratic in the field and is inversely proportional to the detuning of the photons from the resonance frequency (Bakos, 1977; Autler and Townes, 1955).

Whether the photons causing the effect have a greater or lesser energy than the transition energy between the states determines the direction of the shift (Bjorkholm and Liao, 1975; Hurst et al., 1975). If the photon energy is less than the transition energy the dominant term in the denominator $(1/(\omega_r-\omega))$ is positive and the states are pushed apart. A schematic diagram of the process can be found in Figure 5.2. The radiation can be thought of as emanating

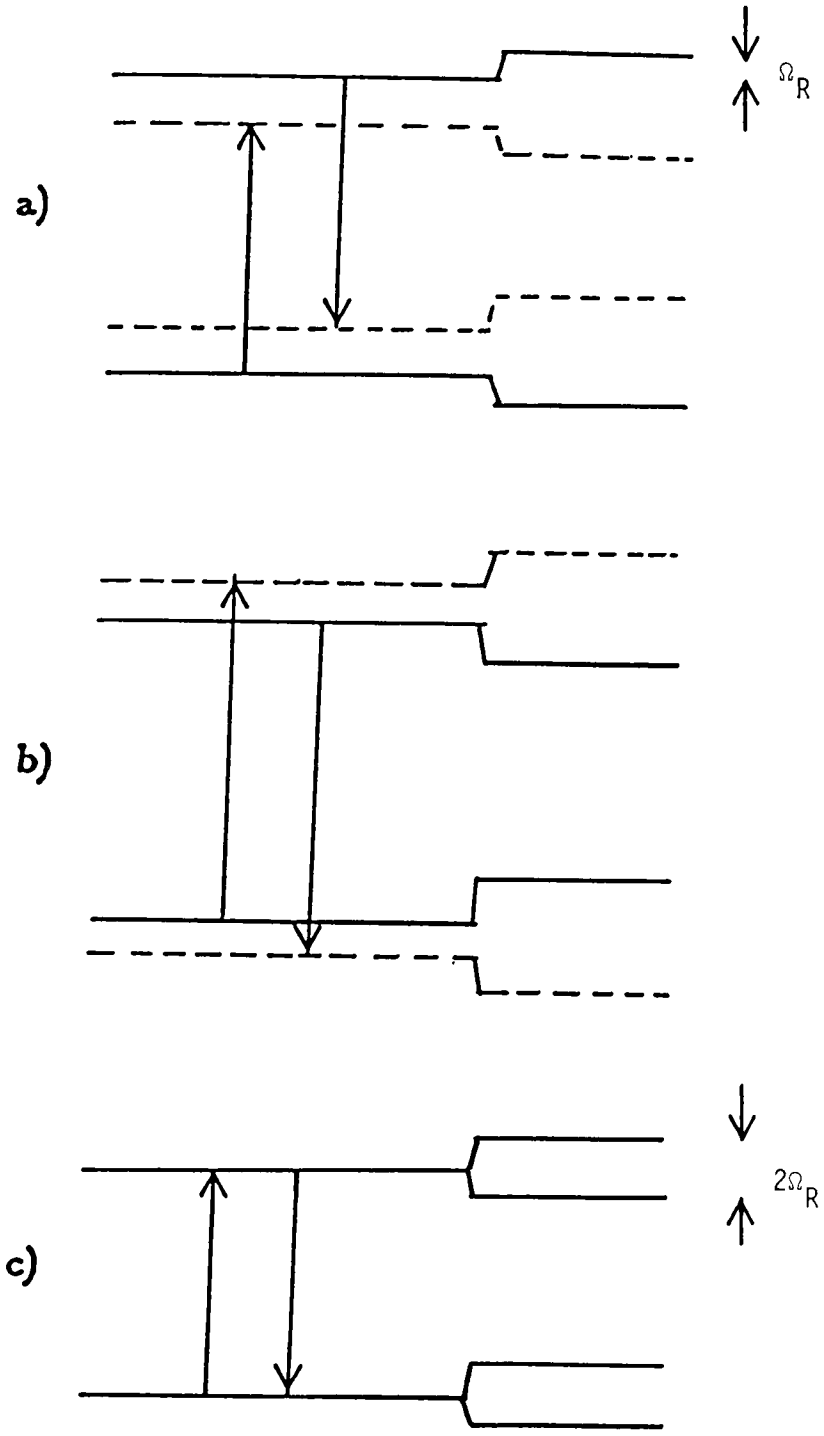

Figure 5.2. The direction of shifts due to the a.c. Stark effect due to direction of photon energy detuning. (a) Low energy detuning causes states to be pushed apart, (b) high energy detuning causes states to be pulled together, and (c) exact resonance causes an apparent splitting of states which is in actuality a rapid oscillation between the energy levels.

from either the upper or lower state. Each direction creates a virtual state (dotted line) that is also shifted. Transitions to these virtual states are much weaker than the actual shifted resonance states, but they may be seen.

If the photon energy is greater than the resonance energy, the states are pulled together since the denominator is negative (Figure 5.2b). The limit of this process is when the radiation is exactly resonant with the transition. The "virtual" states now correspond to the resonance levels and the literature refers to a "splitting of the state" (Autler and Townes, 1955; Bjorkholm and Liao, 1965; Mizushima, 1964). In fact, the a.c. Stark effect may be more appropriately called the Autler-Townes effect since they were the first ones who worked out the details of the process. Although experimentally it appears as though a single state is split, it is actually rapid oscillations between these levels that give that appearance. The oscillation rate is the Rabi frequency and the magnitude of the a.c. Stark splitting is twice the Rabi rate. When a cw laser is used to create the splitting these levels may actually be mapped out. In a pulsed laser system like the one used in all of the experiments described in this study, the Stark shift is smeared into a range from zero (at the beginning and end of a laser pulse) to $2\Omega_R$ (at the peak of laser pulse intensity) where Ω_R is the one-photon Rabi rate between the states. Instead of experimentally observing a distinct splitting one observes a large broadening of the resonance. The a.c. Stark shift (Δ_s) can now be used to explain the backward SHR

emission asymmetry discussed earlier. If one tunes the incident laser to the red (low energy) side of the two-photon 3d resonance (see Figure 5.3a), SHR is emitted between the virtual state and both the $3p_{3/2}$ and $3p_{1/2}$ states, labeled $\omega 1$ and $\omega 2$. If one redraws these transitions from the upper states (dotted lines) it is easily seen that while $\omega 1$ is on the red side of both of the 3d-3p transitions, $\omega 2$ is to the blue side of the $3d\text{-}3p_{3/2}$ transition, but to the red side of the $3d\text{-}3p_{1/2}$ transition. As a result, $\omega 1$ pushes the 3d states away from both of the 3p levels, while $\omega 2$ pushes the $3d\text{-}3p_{1/2}$ levels even further apart, while pushing together the $3d\text{-}3p_{3/2}$. The net effect is to have a total Stark shift which is greater for the $3d\text{-}3p_{1/2}$ transition than it is for the $3d\text{-}3p_{3/2}$ one. Since the Stark shift is larger for the $3d\text{-}3p_{1/2}$ transition, it has a lower transition rate and will, therefore, be suppressed in intensity compared to the case where the laser is tuned exactly to the two-photon resonance. The exact opposite occurs when tuned to the blue (high energy) side of the resonance. Both $\omega 1$ and $\omega 2$ tend to push the $3d\text{-}3p_{3/2}$ states together, while $\omega 1$ pushes the $3d\text{-}3p_{1/2}$ states apart and pulls the $3d\text{-}3p_{3/2}$ levels together. The net effect is to have the Stark shift greater for the $3d\text{-}3p_{3/2}$ transition, and to suppress its transition probability with respect to the $3d\text{-}3p_{1/2}$ emission. Put in other terms, when the laser is detuned to the red side of the two-photon 3d resonance the 8185 Å emission should be more suppressed than the 8197 Å emission when compared to intensities at zero detuning. When detuned to the blue side the opposite should occur.

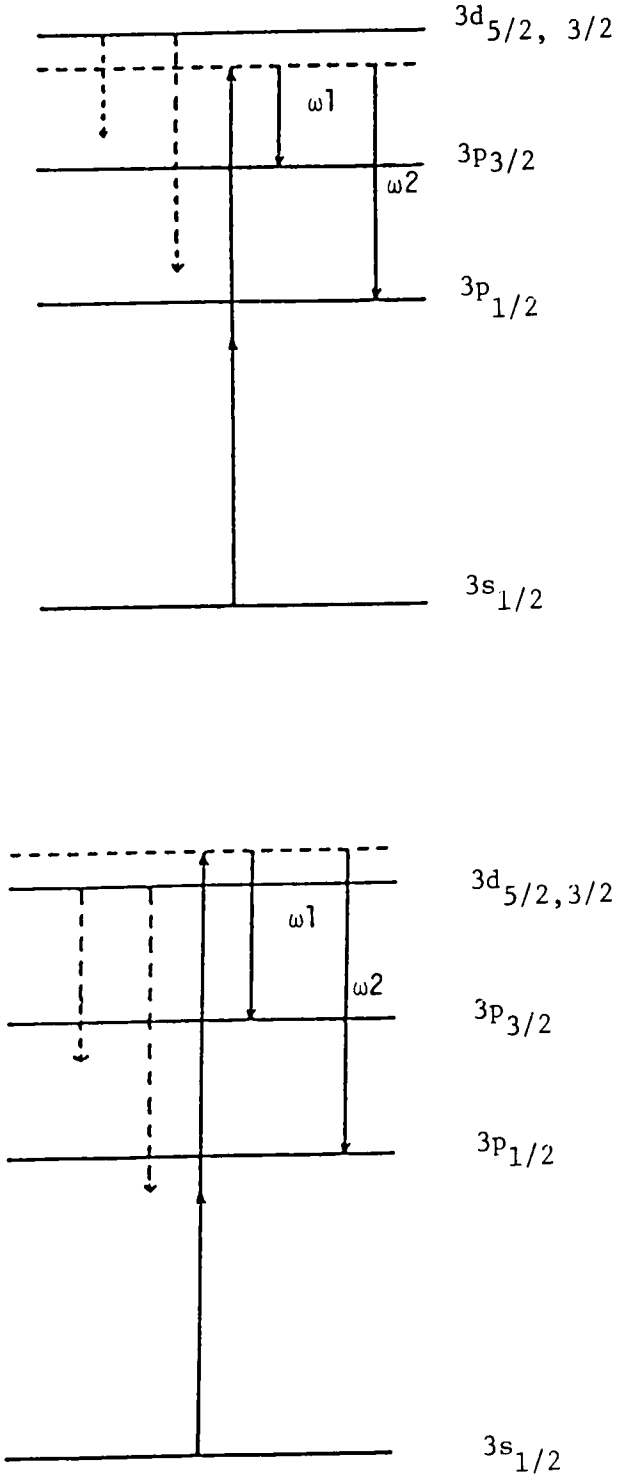

Figure 5.3. Schematic of backward SHR emission out of 3d states illustrating the radiation responsible for the asymmetric suppression of the 3p states as a function of the direction of pump laser detuning due to the a.c. Stark effect.

This is exactly what the wavelength scans in Figure 5.1 show. One expects the intensity of both peaks to be decreased when detuned from resonance, but if one does not include the a.c. Stark effect it is expected that both peaks are affected by the same amount. It is only when one takes the a.c. Stark effect into account that this asymmetry becomes understandable. The a.c. Stark effect in general complicates all studies of atomic resonance phenomena involving strong electromagnetic fields that are near resonance, whether these fields are externally supplied or generated within a nonlinear medium itself. While ignoring the effect greatly simplifies many theoretical problems, it in fact makes the correspondence between theoretical prediction and experimental results less clear.

B. Influence of Population Transfer on Axial PFWM from the Sodium Ground State to Higher Excited States

One of the strong processes observed when tuning the laser to the two-photon 4d resonance is an axially propagating four-wave mixing process (FWM) that involves two laser photons to near the 4d states, an IR photon in the 23,000 Å range that connects the near 4d to near 4p, and a UV photon returning to the 3s ground state (see Figure 5.4). This UV emission is in the 3303 Å range. It has conical components in addition to the axial ones (as explained in Chapter IV), and it propagates only in the forward direction, the direction of the laser photons. The lack of backward UV emission is

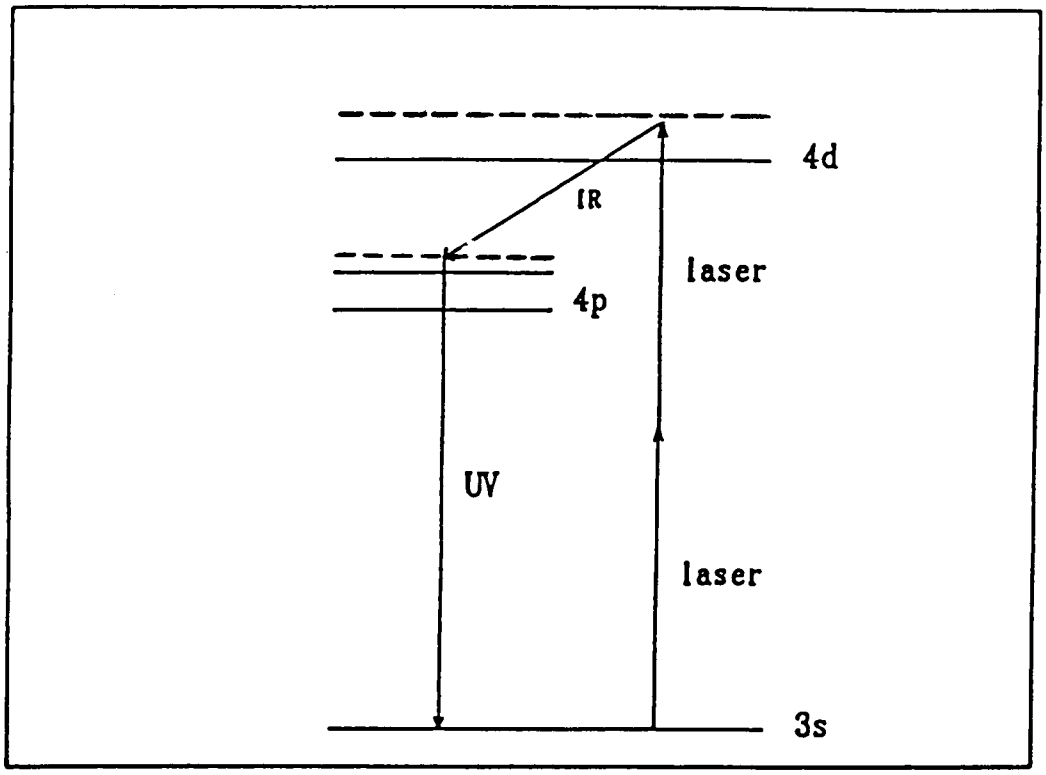

Figure 5.4. Diagram of radiation involved in the production of axially propagating UV PFWM emission out of the 4d state.

strong evidence that a nonresonant FWM process is involved rather than a resonant phenomenon such as ASE or SHR emission. Under certain conditions the axial portion of this UV light displayed a rather unusual behavior. If one counterpropagated two laser beams instead of passing a single beam through the nonlinear medium so that the pulses overlapped in the center of the vapor zone of the heat pipe, one observed that a hole developed in the center of both of the UV beams when tuning across the two-photon 4d resonance. The total UV production went down by a factor of from two to nine depending on vapor pressure and laser intensity.

When the mirrors adjusting the spatial overlap of the beams were adjusted so that no overlap occurred (the beams went through slightly different regions of the sodium vapor), UV production returned to normal. When one of the beams was slightly time delayed so that the spatial overlap of the beams occurred outside of the vapor region, a hole appeared only in the delayed beam. Axial UV production in the first beam to pass through the medium remained at normal intensities.

Spatial profiles of the UV emission were taken by a one-dimensional photodiode array (Reticon) to get relative intensity measurements. These are illustrated in Figure 5.5 where the laser is tuned exactly to the two-photon 4d resonance. Figures 5.5a and 5.5b, taken when the sodium vapor pressure was approximately 5 torr, show a decrease in UV production by a factor of nine between the spatially overlapped and nonoverlapped counterpropagating laser beams. In

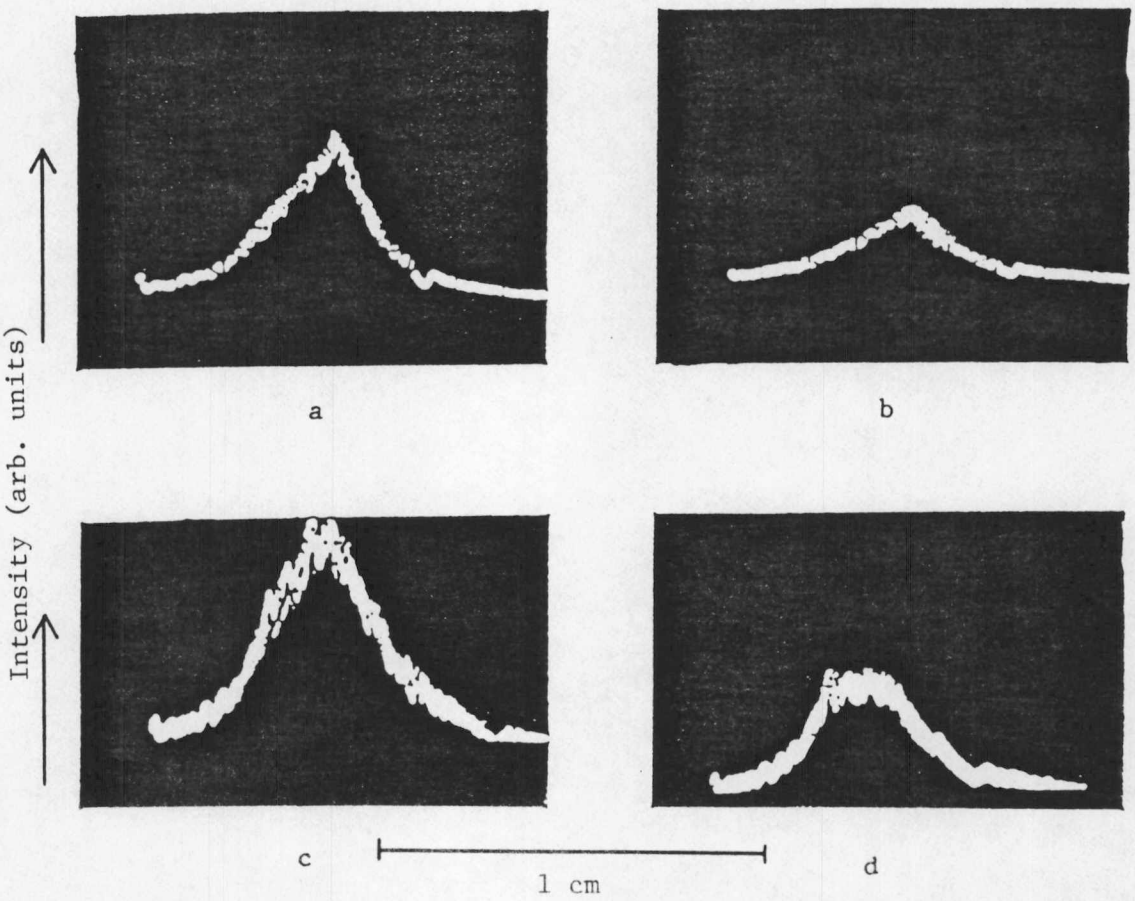

Figure 5.5. Spatial intensity profiles of UV PFWM emission from sodium 4p-3s levels with nonoverlapped and overlapped counterpropagating beams. (a) No overlap, (b) overlapped (scale 2.5 x (a)), P = 5 torr, (c) no overlap, (d) overlapped, P = 2 torr. All figures are to the same horizontal scale.

Figure 5.5c and Figure 5.5d, the pressure is reduced to about two torr and the decrease in UV production is only by a factor of two.

As shown schematically in Figure 5.6, the laser beam is divided into two counterpropagating beams by a 50/50 beam splitter. The beam paths are initially adjusted so that the two beams reach the center of the heat pipe at the same time. A delay line in either direction allowed adjustment of the degree of beam overlap in time, while mirror adjustment controlled spatial overlap.

This study has shown that this severe reduction in UV production when counterpropagating laser beams both spatially and temporally is due to the transfer of population to some state (3p, 4p, 4s, or 3d) other than the ground state (3s). This transfer would change the dispersive qualities of the sodium vapor thereby spoiling the phase-matching conditions necessary for this particular axial FWM to occur.

Evidence for population transfer rather than some other factor such as an interference phenomenon is as follows. If one adjusts the time delay of one of the laser beams, it is possible to get a condition where the initial laser pulse and the counterpropagating pulse do not overlap temporally in the heat pipe vapor region. The laser pulse is approximately 6 ns long, which is equivalent to approximately 180 cm of optical pathlength. If one adds approximately 200 cm to the optical path to one beam, the beams can then be made to counterpropagate, but they will traverse the vapor region at different times. If the sodium atoms return to the ground state after the first pulse

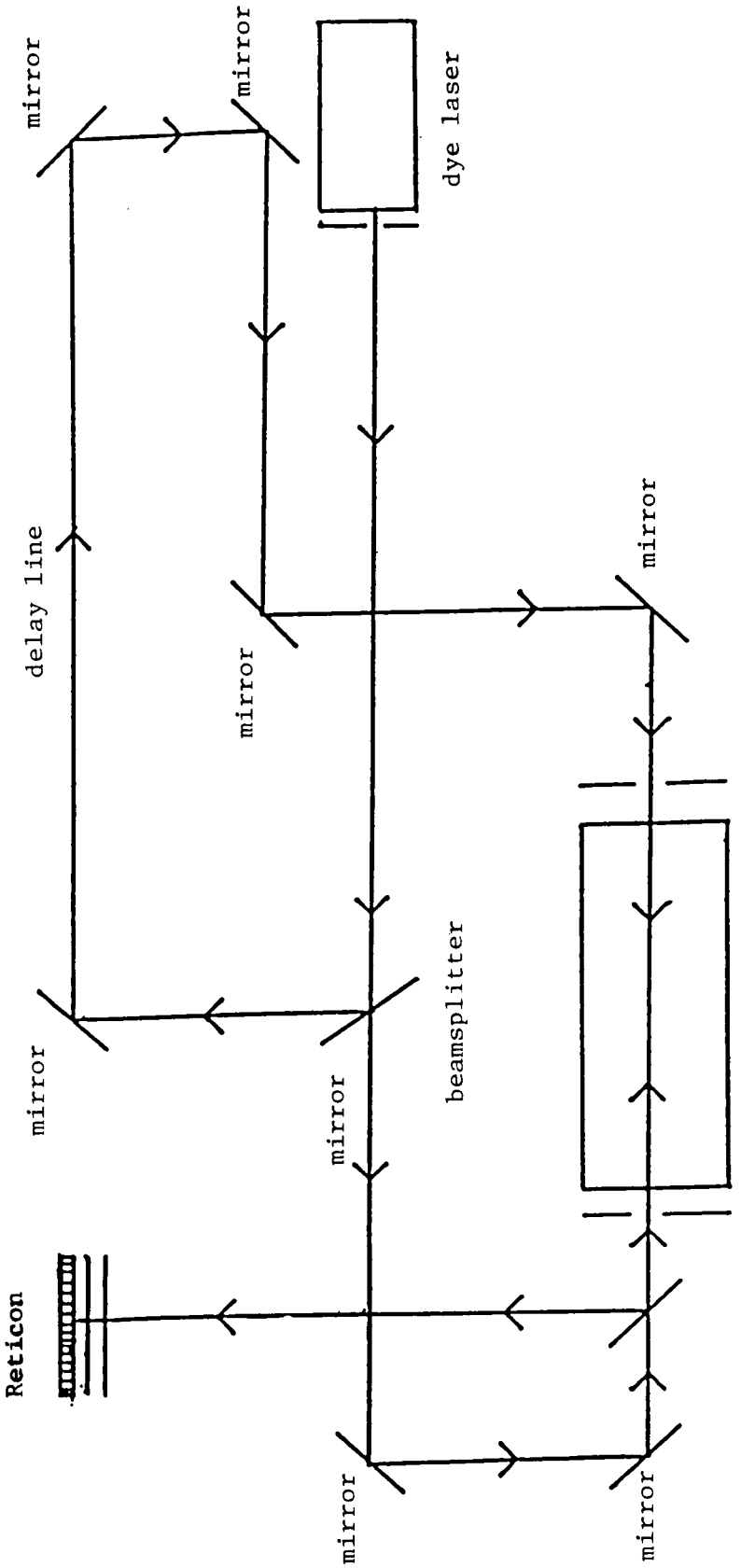

Figure 5.6. Schematic of equipment for a counterpropagating beam experiment.

passes through, one would expect UV production to be the same when the second pulse passes through the medium.

Some decrease in UV intensity in one direction may be expected since the beamsplitter does not give equal intensity at the laser wavelength of 5788 Å. However, since the sodium atoms do not care from which direction the laser photons come, one would expect similar behavior in either direction. Nonresonant processes occur quickly, on the order of 10^{-15} seconds, and persist no longer than the laser pulse itself. In contrast, resonant phenomena may take longer since the electron has a state in which it may remain for a time. In fact, evidence has been found in the case of UV production that nonresonant FWM processes persist on a shorter time scale than the laser pulse length. Measurements with a fast photodiode show that at full width half maximum the laser pulse is $\sim$6 ns long, while the UV pulse is only 4 ns (see Figure 5.7).

When the delay line was put in one of the beams so that the counterpropagating pulses did not overlap in the vapor region, the outcome remained the same as when the initial laser pulse and counterpropagating pulse were overlapped exactly. UV production in the time-delayed direction was diminished by a factor of $\sim$5 or greater.

Because of resonance radiation trapping, the effective lifetime of an electron in an excited state in an alkali can be on the order of microseconds. This is long enough for any atoms that have been transferred to higher energy levels by the initial laser

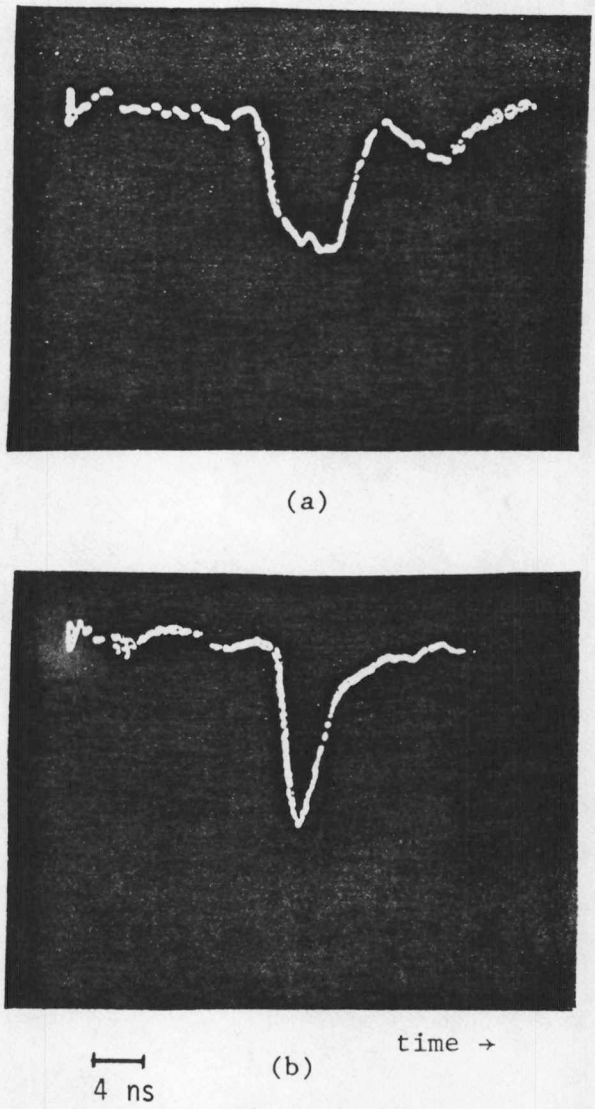

Figure 5.7. Time profiles of pulses taken with a fast photodiode. (a) Laser pulse (FWHM = 6 ns), (b) axially propagating UV PFWM signal (FWHM = 4 ns), P = 2 torr, E = 2 mJ/pulse.

pulse to still be in the higher energy state when the delayed beam passes through. Under these conditions one would not expect axial UV production in the counterpropagating direction. As explained in Chapter IV, population transfer changes the refractive index of the medium and will change the phase-matching point at which axial FWM process will occur. If this point is moved closer to the zero cross-over point where $\chi^{(3)}(\omega)$ is close to zero (see Chapter IV), no polarization source term will exist for the production of the axial UV emission. This experiment provides evidence that under conditions of high vapor pressure and strong laser stimulation that a significant portion of the atoms are transferred out of the ground state. This in turn affects the dispersion of the medium as described in Chapter IV, and may effectively prevent processes that depend on index properties of the medium such as axially phase-matched four-wave mixing.

C. General Conclusions

The total nonlinear response of sodium vapor to laser stimulation is a complicated problem. Although this study has revealed some interesting and new phenomena that can be explained in the context of theoretical models, it has also left many unanswered questions. Processes not included in the preceding experiments include such phenomena as unexplained peaks that may or may not finally be attributed to some secondary nonlinear process induced by frequencies initially produced by the laser photons. There is also the unusual

pressure region around 0.04 torr where the backward SHR from the 3d state exhibits a peak near resonance instead of the characteristic dip seen both at higher and lower pressures caused by the a.c. Stark effect.

The anomalies witnessed when tuning the laser near a one-photon allowed resonance are another topic not pursued here and are left for someone else to pursue. The nonlinear response of sodium vapor has been studied by many experimentalists and theorists over the last few decades, yet a complete model for its behavior is not yet available. There has often been a plethora of unexplained lines and a conspicuous lack of lines that by all accounts should be present. However, this study has illuminated much of the nonlinear response of sodium vapor when stimulated by a laser tuned to or near the two-photon 3d or 4d resonances. It has shown the importance of including the Stark effect in theoretical models that involve resonances. It has demonstrated the suppression of three-photon SHR processes that are also linked by one-photon allowed transitions. It has also shown that four-wave mixing processes do not always have to have a conical emission to obey phase-matching requirements. This study has answered a few questions and raised a few more.

LIST OF REFERENCES

LIST OF REFERENCES

Agarwal, G. S. and S. P. Tewari, Phys. Rev. A 29, 1922 (1984).

Ashfold, M. N. R., C. D. Heryet, J. D. Prince, and B. Tutcher, Chem. Phys. Lett. 131, 291 (1986).

Autler, S. H. and C. H. Townes, Phys. Rev. 100, 703 (1955).

Bakos, J. S., Phys. Lett. Section C 31, 209 (1977).

Baldwin, G. C, An Introduction to Nonlinear Optics (Plenum Press, New York, 1969).

Bjorkholm, J. E. and P. F. Liao, "Optically Induced Atomic Energy Level Shifts and Two-Photon Spectroscopy," Laser Spectroscopy: Proceedings of the Second International Conference, Megeve, June 23-27, 1975, Editors S. Haroche, J. C. Pebay-Peyroula, T. W. Hansch, and S. E. Harris (Berlin; New York; Springer-Verlag, 1975), pp. 176-185.

Bonch-Bruevich, A. M. and V. A. Khodovoi, Sov. Phys. Usp. 10, 637 (1968).

Born, M. and E. Wolf, Principles of Optics, 5th ed. (Pergamon Press, Oxford, 1975).

Boyd, R. W., M. S. Malcuitt, D. J. Gauthier, and K. Rzazewski, Phys. Rev. A 35, 1648 (1987).

Compton, R. N., J. C. Miller, A. E. Carter, and P. Kruit, Chem. Phys. Lett. 71, 87 (1980).

Cotter, D., D. C. Hanna, W. H. W. Tuttlebee, and M. A. Yuratich, Optics Comm. 22, 190 (1977).

Cyvin, S. J., J. E. Rauch, and J. C. Decius, J. of Chem. Phys. 43, 4083 (1965).

Fisher, Robert A., ed., Optical Phase Conjugation (Academic Press, New York, 1983).

Garrett, W. R., W. R. Ferrell, M. G. Payne, and J. C. Miller, Phys. Rev. A 34, 1165 (1986).

Garrett, W. R., S. D. Henderson, and M. G. Payne, Phys. Rev. A 34, 3463 (1986).

Garrett, W. R., S. D. Henderson, and M. G. Payne, Phys. Rev. A 35, 5032 (1987).

Gaupp, Andreas, "Untersuchung der Lebensdauern im Li 2 $^2P_{1/2}$ und Na 3 $^2P_{1/2}$ Zustand Durch Optische Anregung Schneller Atomstrahlen" (Ph.D. dissertation, Freien Universität, Berlin, 1979).

Geller, Y. I. and A. V. Shvabauskas, Optical Spectroscopy (USSR) 53, 227 (1982).

Glownia, J. H. and R. K. Sander, Appl. Phys. Lett. 40, 648 (1982).

Gordon, R. J., Y. T. Lee, and D. R. Herschbach, J. of Chem. Phys. 54, 2393 (1971).

Grischkowsky, D., M. M. T. Loy, and P. F. Liao, Phys. Rev. A 12, 2514 (1975).

Hanna, D. C., M. A. Yuratich, and D. Cotter, Nonlinear Optics of Free Atoms and Molecules (Springer-Verlag, New York, 1979).

Hartig, W., Appl. Phys. 15, 427 (1978).

Hofsaess, D., Zeit. Phys. A 281, 1 (1977).

Hurst, G. S. and M. G. Payne, The Principles and Applications of Resonance Ionisation Spectroscopy (Adam-Helger, Bristol, 1988).

Jackson, D. J. and J. J. Wynne, Phys. Rev. Lett. 49, 543 (1982).

Jackson, D. J. and J. J. Wynne, Proceedings from the XIIth International Quantum Electronics Conference (Munich, n.p., 1982), p. 238.

Jackson, D. J., J. J. Wynne, and P. H. Kes, Phys. Rev. A 28, 781 (1983).

Krasinski, J., D. J. Gauthier, M. S. Malcuitt, and R. W. Boyd, Optics Comm. 54, 241 (1985).

Krasnikov, V. V., M. S. Pshenichnikov, and V. S. Solomatin, JETP Lett. 43, 148 (1986).

Li, L, M. Wu, and P. M. Johnson, J. Chem. Phys. 86, 1131 (1987).

Louisell, W. H. and P. Meystre, Phys. Rev. A 23, 1015 (1981).

Malcuitt, M. S., D. J. Gauthier, and R. W. Boyd, Phys. Rev. Lett. 55, 1086 (1985).

Manykin, E. A. and A. M. Afanasev, Soviet Physics JETP 21, 619 (1965).

Manykin, E. A. and A. M. Afanasev, Soviety Physics JETP 25, 828 (1967).

McDaniel, E., Collision Phenomena in Ionized Gases (John Wiley and Sons, Inc., New York, 1964).

Miller, J. C., R. N. Compton, M. G. Payne, and W. R. Garrett, Phys. Rev. Lett. 45, 114 (1980).

Miller, John C. and R. N. Compton, Phys. Rev. A 25, 2056 (1982).

Mizushima, M., Phys. Rev. A 133, 414 (1964).

Moore, C. E., Atomic Energy Levels, Vol. I (National Bureau of Standards, NSRDS-NBS 35, 1971).

Moore, M. A., W. R. Garrett, and M. G. Payne, "Suppression of Electronic Hyper-Raman Emission by Four-Wave Mixing" (to be published, 1988).

Normand, D., J. Morellec, and J. Reif, J. of Phys. B 16, L227 (1983).

Orlando, T. M., L. Li, S. L. Anderson, and M. G. White, Chem. Phys. Lett. 129, 31 (1986).

Payne, M. G., private communication (1988).

Payne, M. G. and W. R. Garrett, Phys. Rev. A 26, 356 (1982).

Payne, M. G. and W. R. Garrett, Phys. Rev. A 28, 3409 (1983).

Payne, M. G., W. R. Garrett, and H. C. Baker, Chem. Phys. Lett. 75, 468 (1980).

Payne, M. G., W. R. Garrett, and W. R. Ferrell, Phys. Rev. A 34, 1143 (1986).

Payne, M. G., W. R. Garrett, M. A. Moore, and R. Wunderlich, "New Effects Relating to the Hyper Raman Process" (to be published, 1988).

Sargent, M., M. O. Scully, and W. E. Lamb, Laser Physics (Addison-Wesley Publishing Co., Reading, MA, 1974).

Shen, Y. R., The Principles of Nonlinear Optics (John Wiley and Sons, Inc., New York, 1984).

Terhune, R. W., P. D. Maker, and G. M. Savage, Phys. Rev. Lett. 14, 681 (1965).

Vrehen, Q. H. F. and H. M. J. Hikspoor, Optics Comm. 22, 127 (1977).

Weise, W. L., M. W. Smith, and B. M. Miles, Atomic Transition Probabilities, Vol. 2 (National Bureau of Standards, NSRDS-NBS22, 1969).

Wynne, J. J., Phys. Rev. Lett. 52, 751 (1984).

VITA

Mary Anne Kozilsky Moore was born in Troy, New York, on August 31, 1951. At the age of six she moved to the town of Rotterdam, near Schenectady, New York, and attended local schools. She attended the Crane School of Music at the State University College of Potsdam, New York, and received a B.M. in music education in 1973.

She taught string music in the Cortland, New York, city schools before moving to Knoxville, Tennessee, in 1974. There she taught violin and viola privately, played in the Knoxville Symphony, and earned an M.S. in music education from The University of Tennessee, Knoxville.

In 1979 she decided to pursue a course of study in physics at The University of Tennessee, receiving a B.A. in 1983 and a Ph.D. in 1988. During this time she has pursued an avid interest in astronomy and enjoyed her research experience in Photophysics Section at the Oak Ridge National Laboratory.